

# ANALYSIS OF THE CRACKED INFINITE HOLLOW CYLINDER WITH LOADING ON CRACK SURFACES

A Thesis Submitted to  
the Graduate School of Engineering and Sciences of  
İzmir Institute of Technology  
in Partial Fulfilment of the Requirements for the Degree of  
  
MASTER SCIENCE  
  
in Mechanical Engineering

by  
Fatih AVCI

March, 2009  
İZMİR

We approve the thesis of **Fatih AVCI**

---

Asst. Prof. Dr. H. Seil ALTUNDAĐ ARTEM  
Supervisor

---

Asst. Prof. Dr. Ebubekir ATAN  
Committee Member

---

Assoc Prof. Dr. M. Evren TOYGAR  
Committee Member

17 March 2009

---

Assoc. Prof. Dr. Metin TANOĐLU  
Head of the Mechanical Engineering  
Department

---

Prof. Dr. Hasan BÖKE  
Dean of the Graduate School of  
Engineering and Sciences

## **ACKNOWLEDGMENTS**

I would like to express my gratitude to my supervisor, Asst. Prof. Dr. H. Seil Altundađ Artem, whose expertise, understanding, support and patience added considerably to my graduate experience.

I would also like to thank my family for the support and help they provided me during the course of this study.

Finally, I would like to thank Levent Aydın for his help and comments.

# **ABSTRACT**

## **ANALYSIS OF THE CRACKED INFINITE HOLLOW CYLINDER WITH LOADING ON CRACK SURFACES**

In this study, the cracked infinite hollow cylinder with an axisymmetric crack of width  $(b-a)$  is considered. The ring-shaped crack is located at the symmetry plane. Surfaces of the crack are subjected to the distributed compressive loads. The outer surface of the cylinder is rigid and the inner one is stress free. The material of the cylinder is assumed to be linearly elastic and isotropic.

Integral transform techniques are used for the solution of the field equations. The resultant singular integral equation in terms of crack surface displacement derivative is converted to a system of linear algebraic equations by using Gauss-Lobatto, Gauss-Jacobi and Gauss-Laguerre integration formulas. The stress intensity factors at the tips of the crack are numerically calculated for uniform and linear load distributions on crack surfaces. Some results are presented in graphical and tabular forms.

# ÖZET

## ÇATLAK YÜZEYLERİNDE YÜKE MARUZ SONSUZ UZUNLUKTAKİ TÜPÜN ANALİZİ

Bu çalışmada, eni  $(b-a)$  olan aksenal simetrik çatlak içeren sonsuz uzunlukta bir tüp problemi ele alınmıştır. Halka biçimindeki çatlak simetri düzleminde yer almaktadır. Çatlak yüzeyleri yayılı basınç yüklerine maruzdur. Tüpün dış yüzeyi rijit, iç yüzeyi serbesttir. Tüpün malzemesi lineer elastik ve izotrop olduğu varsayılmaktadır.

Elastisite denklemlerinin çözümü için integral dönüşüm teknikleri kullanıldı. Gauss-Lobatto, Gauss-Jacobi ve Gauss Laguerre integrasyon formülleri kullanılarak, çatlak yüzü yer değiştirme türevi cinsinden yazılan tekil integral denklemi bir lineer cebrik denklem takımına dönüştürülmüştür. Düzgün ve lineer yayılı basınç yükleri için çatlak uçlarındaki gerilme şiddeti katsayıları nümerik olarak hesaplandı. Bazı sonuçlar grafikler ve tablolar biçiminde verilmektedir.

# TABLE OF CONTENTS

LIST OF FIGURES.....	viii
LIST OF TABLES.....	xi
CHAPTER 1. INTRODUCTION.....	1
1.1. A Brief Introduction and Method of Solution.....	2
1.2. Literature Overview.....	2
CHAPTER 2. PROBLEM DEFINITION AND FORMULATION.....	5
2.1. The Infinite Hollow Cylinder Containing a Ring-Shaped Crack Problem.....	5
2.1.1. The Perturbation Problem.....	8
2.1.1.1. An Infinite Elastic Medium having a Crack.....	8
2.1.1.2. An Infinite Elastic Medium without a Crack.....	12
2.1.2. General Solution.....	14
CHAPTER 3. SOLUTION OF THE INTEGRAL EQUATIONS.....	18
3.1. Derivation of the Integral Equation.....	18
3.2. Characteristic Equation.....	21
3.2.1. Internal Crack.....	23
3.2.2. Crack Terminating at Rigid Surface.....	23
3.2.3. Internal Edge Crack.....	24
3.3. Solution of the Integral Equation.....	24
3.3.1. Internal Crack.....	25
3.3.2. Crack Terminating at Rigid Surface.....	26
3.4. Stress Intensity Factors.....	27
3.4.1. Stress Intensity Factors at the Tips of Internal Crack.....	27
3.4.2. Stress Intensity Factors at the Tips of Crack Terminating at Rigid Surface.....	29
3.4.3. Stress Intensity Factor at the Tip of Internal Edge Crack.....	30
CHAPTER 4. NUMERICAL RESULTS AND DISCUSSION.....	31

CHAPTER 5. CONCLUSION.....	52
REFERENCES.....	53
APPENDICES	
APPENDIX A. INTEGRATION FORMULAS.....	55
APPENDIX B. INTEGRAL FORMS AND COEFFICIENTS.....	57
APPENDIX C. ASYMPTOTIC EXPANSIONS.....	62
APPENDIX D. ALGEBRAIC EQUALITIES.....	64
APPENDIX E. GAUSS-LOBATTO AND GAUSS-LAGUERRE INTEGRATION.....	65

# LIST OF FIGURES

<b><u>Figure</u></b>	<b><u>Page</u></b>
Figure 1.1. Three modes of application of the load.....	1
Figure 2.1. Geometry of the problem.....	5
Figure 2.2. Perturbation problem.....	8
Figure 4.1. Variation of the normalized stress intensity factor $\overline{k}_1(a)$ for an internal crack in the thick-walled cylinder ( $A/B = 0.25$ ) for load distribution of $p_0(r) = p_0$ .....	33
Figure 4.2. Variation of the normalized stress intensity factor $\overline{k}_1(b)$ for an internal crack in the thick-walled cylinder ( $A/B = 0.25$ ) for load distribution of $p_0(r) = p_0$ .....	34
Figure 4.3. Variation of the normalized stress intensity factor $\overline{k}_1(a)$ for an internal crack in the thick-walled cylinder ( $A/B = 0.25$ ) for load distribution of $p_1(r) = \frac{3(b^2-a^2)(r-B)}{2b^3-3Bb^2-2a^3+3Ba^2} p_0$ .....	34
Figure 4.4. Variation of the normalized stress intensity factor $\overline{k}_1(b)$ for an internal crack in the thick-walled cylinder ( $A/B = 0.25$ ) for load distribution of $p_1(r) = \frac{3(b^2-a^2)(r-B)}{2b^3-3Bb^2-2a^3+3Ba^2} p_0$ .....	35
Figure 4.5. Variation of the normalized stress intensity factor $\overline{k}_1(a)$ for an internal crack in the thick-walled cylinder ( $A/B = 0.25$ , $\nu = 0.3$ ) for load distributions of $p_0(r) = p_0$ and $p_1(r) = \frac{3(b^2-a^2)(r-B)}{2b^3-3Bb^2-2a^3+3Ba^2} p_0$ .....	36
Figure 4.6. Variation of the normalized stress intensity factor $\overline{k}_1(b)$ for an internal crack in the thick-walled cylinder ( $A/B = 0.25$ , $\nu = 0.3$ ) for load distributions of $p_0(r) = p_0$ and $p_1(r) = \frac{3(b^2-a^2)(r-B)}{2b^3-3Bb^2-2a^3+3Ba^2} p_0$ .....	36
Figure 4.7. Variation of the normalized stress intensity factor $\overline{k}_1(a)$ for an internal crack in the thick-walled cylinder ( $A/B = 0.25$ , $a/A = 1.6$ ) for uniform load distribution of $p_0(r) = p_0$ .....	37



Figure 4.8. Variation of the normalized stress intensity factor $\bar{k}_1(b)$ for an internal crack in the thick-walled cylinder ( $A/B = 0.25$ , $a/A = 1.6$ ) for uniform load distribution of $p_0(r) = p_0$ .....	38
Figure 4.9. Variation of the normalized stress intensity factor $\bar{k}_1(a)$ for an internal crack in the thick-walled cylinder ( $A/B = 0.25$ , $a/A = 1.6$ ) for load distribution of $p_1(r) = \frac{3(b^2-a^2)(r-B)}{2b^3-3Bb^2-2a^3+3Ba^2} p_0$ .....	38
Figure 4.10. Variation of the normalized stress intensity factor $\bar{k}_1(b)$ for an internal crack in the thick-walled cylinder ( $A/B = 0.25$ , $a/A = 1.6$ ) for load distribution of $p_1(r) = \frac{3(b^2-a^2)(r-B)}{2b^3-3Bb^2-2a^3+3Ba^2} p_0$ .....	39
Figure 4.11. Variation of the normalized stress intensity factor $\bar{k}_1(a)$ for an internal crack in the thick-walled cylinder ( $A/B = 0.25$ , $v = 0.3$ , $a/A = 1.6$ ) for load distributions of $p_0(r) = p_0$ and $p_1(r) = \frac{3(b^2-a^2)(r-B)}{2b^3-3Bb^2-2a^3+3Ba^2} p_0$ .....	40
Figure 4.12. Variation of the normalized stress intensity factor $\bar{k}_1(b)$ for an internal crack in the thick-walled cylinder ( $A/B = 0.25$ , $v = 0.3$ , $a/A = 1.6$ ) for load distributions of $p_0(r) = p_0$ and $p_1(r) = \frac{3(b^2-a^2)(r-B)}{2b^3-3Bb^2-2a^3+3Ba^2} p_0$ .....	40
Figure 4.13. Variation of the normalized stress intensity factor $\bar{k}_1(a)$ for an internal crack in the thick-walled cylinder ( $A/B = 0.25$ , $b/A = 3.4$ ) for uniform load distribution of $p_0(r) = p_0$ .....	41
Figure 4.14. Variation of the normalized stress intensity factor $\bar{k}_1(b)$ for an internal crack in the thick-walled cylinder ( $A/B = 0.25$ , $b/A = 3.4$ ) for uniform load distribution of $p_0(r) = p_0$ .....	42
Figure 4.15. Variation of the normalized stress intensity factor $\bar{k}_1(a)$ for an internal crack in the thick-walled cylinder ( $A/B = 0.25$ , $b/A = 3.4$ ) for load distribution of $p_1(r) = \frac{3(b^2-a^2)(r-B)}{2b^3-3Bb^2-2a^3+3Ba^2} p_0$ .....	42
Figure 4.16. Variation of the normalized stress intensity factor $\bar{k}_1(b)$ for an internal crack in the thick-walled cylinder ( $A/B = 0.25$ , $b/A = 3.4$ ) for load distribution of $p_1(r) = \frac{3(b^2-a^2)(r-B)}{2b^3-3Bb^2-2a^3+3Ba^2} p_0$ .....	43
Figure 4.17. Variation of the normalized stress intensity factor $\bar{k}_1(a)$ for an internal crack in the thick-walled cylinder ( $A/B = 0.25$ , $v = 0.3$ , $b/A = 3.4$ ) for load distributions of $p_0(r) = p_0$ and $p_1(r) = \frac{3(b^2-a^2)(r-B)}{2b^3-3Bb^2-2a^3+3Ba^2} p_0$ .....	44

- Figure 4.18. Variation of the normalized stress intensity factor  $\bar{k}_1(b)$  for an internal crack in the thick-walled cylinder ( $A/B = 0.25$ ,  $\nu = 0.3$ ,  $b/A = 3.4$ ) for load distributions of  $p_0(r) = p_0$  and  $p_1(r) = \frac{3(b^2-a^2)(r-B)}{2b^3-3Bb^2-2a^3+3Ba^2} p_0$ .....44
- Figure 4.19. Variation of the normalized stress intensity factor  $\bar{k}_1(a)$  for a crack terminating at rigid surface in the thick-walled cylinder ( $A/B = 0.25$ ,  $b/B = 1$ ) for load distribution of  $p_0(r) = p_0$ .....45
- Figure 4.20. Variation of the normalized stress intensity factor  $\bar{k}_1(b)$  for a crack terminating at rigid surface in the thick-walled cylinder ( $A/B = 0.25$ ,  $b/B = 1$ ) for load distribution of  $p_0(r) = p_0$ .....46
- Figure 4.21. Variation of the normalized stress intensity factor  $\bar{k}_1(a)$  for a crack terminating at rigid surface in the thick-walled cylinder ( $A/B = 0.25$ ,  $b/B = 1$ ) for load distribution of  $p_1(r) = \frac{3(b^2-a^2)(r-B)}{2b^3-3Bb^2-2a^3+3Ba^2} p_0$ .....46
- Figure 4.22. Variation of the normalized stress intensity factor  $\bar{k}_1(b)$  for a crack terminating at rigid surface in the thick-walled cylinder ( $A/B = 0.25$ ,  $b/B = 1$ ) for load distribution of  $p_1(r) = \frac{3(b^2-a^2)(r-B)}{2b^3-3Bb^2-2a^3+3Ba^2} p_0$ .....47
- Figure 4.23. Variation of the normalized stress intensity factor  $\bar{k}_1(a)$  for a crack terminating at rigid surface ( $A/B = 0.25$ ,  $\nu = 0.3$ ,  $b/B = 1$ ) for load distributions of  $p_0(r) = p_0$  and  $p_1(r) = \frac{3(b^2-a^2)(r-B)}{2b^3-3Bb^2-2a^3+3Ba^2} p_0$ .....48
- Figure 4.24. Variation of the normalized stress intensity factor  $\bar{k}_1(b)$  for a crack terminating at rigid surface ( $A/B = 0.25$ ,  $\nu = 0.3$ ,  $b/B = 1$ ) for load distributions of  $p_0(r) = p_0$  and  $p_1(r) = \frac{3(b^2-a^2)(r-B)}{2b^3-3Bb^2-2a^3+3Ba^2} p_0$ .....48
- Figure 4.25. Variation of the normalized stress intensity factor  $\bar{k}_1(b)$  for an internal edge crack in the thick-walled cylinder ( $A/B = 0.25$ ,  $a/A = 1$ ) for load distribution of  $p_0(r) = p_0$ .....49
- Figure 4.26. Variation of the normalized stress intensity factor  $\bar{k}_1(b)$  for an internal edge crack in the thick-walled cylinder ( $A/B = 0.25$ ,  $a/A = 1$ ) for load distribution of  $p_1(r) = \frac{3(b^2-a^2)(r-B)}{2b^3-3Bb^2-2a^3+3Ba^2} p_0$ .....50
- Figure 4.27. Variation of the normalized stress intensity factor  $\bar{k}_1(b)$  for an internal edge crack in the thick-walled cylinder ( $A/B = 0.25$ ,  $\nu = 0.3$ ,  $a/A = 1$ ) for load distributions of  $p_0(r) = p_0$  and  $p_1(r) = \frac{3(b^2-a^2)(r-B)}{2b^3-3Bb^2-2a^3+3Ba^2} p_0$ .....51

# LIST OF TABLES

<b><u>Table</u></b>	<b><u>Page</u></b>
Table 4.1. Variation of the normalized stress intensity factors for an internal crack in the thick-walled cylinder ( $A/B = 0.25, \nu = 0.3$ ) for load distribution of $p_0(r) = p_0$ .....	32

# CHAPTER 1

## INTRODUCTION

An important step is the identification of the most likely modes of failure and the application of a suitable failure criterion in the design of structural or machine components. Fracture characterized as the formation of new surfaces in the material is one such mode of mechanical failure. Fracture may be viewed as the rupture separation of the structural component into two or more pieces due to the discontinuities. These discontinuities can be in the form of cracks, holes, notches or inclusions that are very important factors influencing stress distributions in the structural or machine components.

There are two approaches to fracture study. The first is based on the *stress intensity factor*,  $k$  and the second is based on the *J integral*. The *J integral* approach is suitable for ductile fracture with strong deformations. The *stress intensity factor* approach is based on the possibility of representing the stress field around the crack tip by a *stress intensity factor*,  $k$ . The *stress intensity factor* depends on the way the crack is invited to propagate, on the mode of application of the load, on the level and variation of the stress in the material far from the crack tip and on the type of the crack. These modes of application of the load are defined as of three types (Figure 1.1.):

- *Mode I*: the principle load is applied normal to the crack plane, tends to open crack
- *Mode II*: corresponds to in plane shear loading, tends to slide one crack face with respect to the other one
- *Mode III*: refers to out of plane shear loading.

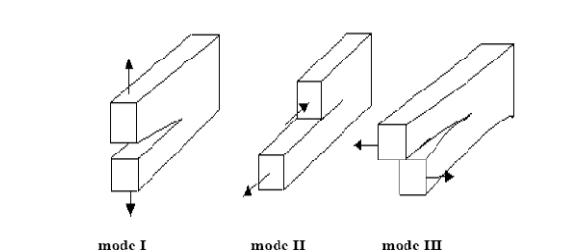


Figure 1.1. Three modes of application of the load.

The stress becomes infinite at the tips of the cracks or inclusions. In such cases, stress concentration cannot be defined as a strength parameter and it is necessary to consider the stress distributions from fracture mechanics point of view. Fracture toughness can be easily calculated in terms of the *stress intensity factors*. The stress near the crack tip varies with singularity, regardless of the configuration of the cracked body. These types of problems are studied by using numerical and analytical methods based on partial differential equations. For linear elastic materials, individual components of stress, strain and displacement are additive. In many cases of analytical solutions, principle of superposition allows stress intensity for complex configurations to be built from simple cases.

### **1.1. A Brief Introduction and Method of Solution of the Problem**

In this study, an infinite hollow cylinder containing a ring-shaped crack at the symmetry plane is considered. Crack surfaces are subjected to distributed load. The outer wall of the hollow cylinder is rigid and the inner wall is free of traction. The material of the hollow cylinder is assumed to be linearly isotropic and elastic. The solution for the problem can be found by superposition of two sub-problems: (1) the problem of an infinite elastic medium containing a ring-shaped crack at the symmetry plane and (2) the problem of an infinite elastic medium without a crack subjected to arbitrary symmetric loads.

The general solutions of these sub-problems are obtained by using Hankel and Fourier transforms on Navier equations. And a singular integral equation is obtained by using the boundary conditions on the crack. By using Gauss-Lobatto and Gauss-Jacobi integration formulas, this singular integral equation is reduced to a linear algebraic equation. And this linear algebraic equation is solved numerically by using Gauss-Laguerre integration.

### **1.2. Literature Overview**

Collins (1962) considered some axially symmetric stress distributions in an infinite elastic solid and in a thick plate containing penny-shape cracks. It was shown that representations for the displacements in an infinite solid containing two or more

cracks and in a thick plate containing a single crack can be constructed and used to reduce problems of determining the stresses in these solids to the solutions of Fredholm integral equations of the second kind by use of representation for the displacement in an infinite elastic solid containing a single crack.

Sneddon and Welch (1963) considered a long circular cylinder of elastic material and made an analysis of the distribution of stress when it is deformed by the application of pressure to the inner surfaces of a penny-shaped crack positioned symmetrically at the centre of the cylinder. The cylinder surface was assumed to be free from stress. The equations of the classical theory of elasticity were solved in terms of an unknown function that was shown to be the solution of an integral solution previously derived by Collins (1962).

Arin and Erdoğan (1971) considered two axially symmetric mixed boundary value problems in elastic dissimilar layered medium. An elastic layer was assumed to be bonded to two semi-infinite half spaces along its plane surfaces, and contains a penny-shape crack parallel to the interfaces. The numerical examples were given for a constant pressure on the crack surface.

The axisymmetric semi-infinite cylinder with fixed short end is considered by Gupta (1974). Normal loads were applied far away from the fixed end. By using an integral transform technique, a singular integral equation has been provided. Stress along the rigid end and stress intensity factors have been calculated numerically and presented graphically.

Agarwal (1978) reduced the axisymmetric end-problem for semi-infinite elastic circular cylinder to a system of singular integral equations. It is found that the kernels of the integral equations contained Cauchy as well as generalized Cauchy-type singularities. A system of algebraic equations was obtained from the system of singular integral equations by using an approximate method. Axisymmetric solution for joined dissimilar elastic semi-infinite cylinders under uniform tension was solved as an application.

Erdöl and Erdoğan (1978) studied an elastostatic axisymmetric problem for a long thick-walled cylinder containing a ring-shaped internal or edge crack. The problem had been formulated in terms of an integral equation has a simple Cauchy kernel for the internal crack and a generalized Cauchy kernel for edge crack as dominant part by using transform technique.

Nied and Erdoğan (1983) considered the elasticity problem for a long hollow cylinder containing an axisymmetric circumferential crack subjected to general non-axisymmetric external loads. The problem had been formulated in terms of a system of singular integral equations. Stress intensity factors and the crack opening displacement had been calculated for a cylinder under uniform tension.

Chen (2000) evaluated the stress intensity factors in a cylinder with a circumferential crack. To study the problem, an indirect method has been developed. The finite difference method had been used to solve the boundary value problem. Numerical examples had been given which demonstrates the effect of cylinder length on the stress intensity factor.

Artem and Geçit (2002) studied the problem of an elastic hollow cylinder under axial tension containing a crack and two rigid inclusions of ring shape. The material of the hollow cylinder was assumed to be linearly elastic and isotropic. The cylinder was assumed to be under the action of uniform loading. Because of the mixed boundary condition of the problem, Hankel and Fourier transform techniques were used and a system of three singular integral equations is analyzed and solved numerically. The normalized stress intensity factors were calculated for crack and two rigid inclusions.

Aydın (2005) made an investigation of stress intensity factors in an elastic cylinder under axial tension with a crack of ring-shape. Hankel and Fourier transform techniques were used to obtain a singular integral equation. This singular integral equation was solved numerically by using Gauss-Lobatto integration formula. The normalized stress intensity factors were calculated for crack and presented graphically.

Kaman and Geçit (2006) considered the problems of cracked semi-infinite cylinder and finite cylinder. General solutions of these problems were obtained by using Hankel and Fourier transforms on Navier equations. The singular integral equations were converted to a system of linear algebraic equations that were solved numerically by using Gauss-Lobatto and Gauss-Jacobi integration formulas. Mode I and Mode II stress intensity factors at the edges of cracks and inclusion and normal and shearing stresses along the rigid support were calculated. And results were presented graphically.

## CHAPTER 2

### PROBLEM DEFINITION AND FORMULATION

#### 2.1. The Infinite Hollow Cylinder Containing a Ring-Shaped Crack Problem

An infinite hollow cylinder of width  $(B-A)$  containing a ring-shaped crack of width  $(b-a)$  at the symmetry plane,  $z = 0$  is considered. Distributed compressive load is applied on the crack surface. The outer wall of the cylinder is rigid and the inner wall is free of traction. The material of the cylinder is assumed to be linearly elastic and isotropic (Figure 2.1).

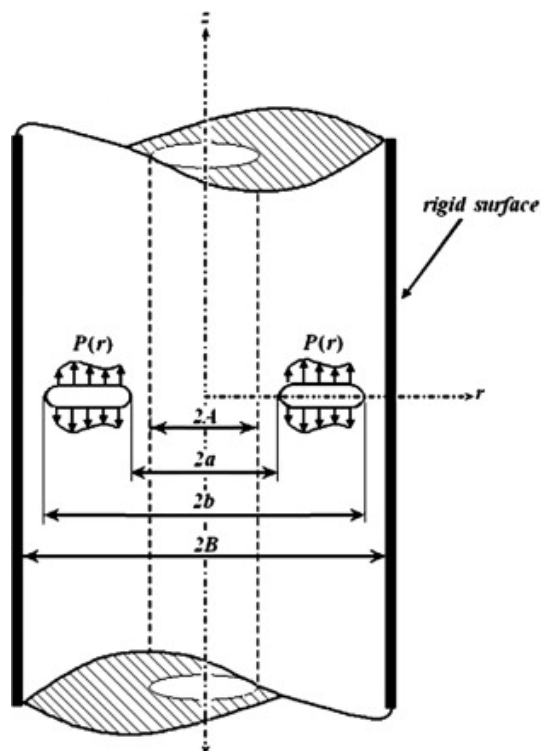


Figure 2.1. Geometry of the problem



The equilibrium equations for linearly elastic, isotropic and axisymmetric problems can be written in the form of

$$\frac{\partial \sigma_r}{\partial r} + \frac{\partial \tau_{rz}}{\partial z} + \frac{\sigma_r - \sigma_\theta}{r} = 0 \quad (2.1)$$

$$\frac{\partial \tau_{rz}}{\partial r} + \frac{\partial \sigma_z}{\partial z} + \frac{\tau_{rz}}{r} = 0 \quad (2.2)$$

where  $\sigma$  and  $\tau$  symbolizes the normal and shear stresses, respectively. The relation between stress and strain in the body in tensor notation is

$$\sigma_{ij} = 2\mu\epsilon_{ij} + \lambda\epsilon_{kk}\delta_{ij} \quad (2.3)$$

where

$$\delta_{ij} = \begin{cases} 1 & \text{for } i = j \\ 0 & \text{for } i \neq j \end{cases}$$

$$\epsilon_{kk} = \epsilon_{rr} + \epsilon_{\theta\theta} + \epsilon_{zz}$$

$$\lambda = \mu \frac{2\nu}{1-2\nu}$$

and  $\mu$  is the shear modulus,  $\nu$  is the Poisson's ratio.

The strain-displacement relations for the axisymmetric problem are in the form of

$$\begin{aligned} \epsilon_{rr} &= \frac{\partial u}{\partial r} \\ \epsilon_{\theta\theta} &= \frac{u}{r} \\ \epsilon_{zz} &= \frac{\partial w}{\partial z} \\ \epsilon_{rz} &= \frac{\partial u}{\partial z} + \frac{\partial w}{\partial r} \end{aligned} \quad (2.4a-d)$$

where  $u$  and  $w$  are displacements in  $r$  and  $z$  directions in cylindrical coordinates, respectively.

By substituting expressions given in the equation (2.4a-d) into the equation (2.3), stress-displacement relations for the axisymmetric cylindrical problem are found as

$$\begin{aligned}
\sigma_r &= \frac{\mu}{K-1} \left[ (K+1) \frac{\partial u}{\partial r} + (3-K) \left( \frac{u}{r} + \frac{\partial w}{\partial z} \right) \right] \\
\sigma_\theta &= \frac{\mu}{K-1} \left[ (K+1) \frac{u}{r} + (3-K) \left( \frac{\partial u}{\partial r} + \frac{\partial w}{\partial z} \right) \right] \\
\sigma_z &= \frac{\mu}{K-1} \left[ (K+1) \frac{\partial w}{\partial z} + (3-K) \left( \frac{\partial u}{\partial r} + \frac{u}{r} \right) \right] \\
\tau_{rz} &= \mu \left( \frac{\partial u}{\partial z} + \frac{\partial w}{\partial r} \right)
\end{aligned} \tag{2.5a-d}$$

where  $K = 3 - 4\nu$  for plane strain.

By substituting equations (2.5a-d) into the equations (2.1) and (2.2), a second order partial differential equation system that is called *the Navier Equations* can be found as

$$\begin{aligned}
(K+1) \left( \frac{\partial^2 u}{\partial r^2} + \frac{1}{r} \frac{\partial u}{\partial r} - \frac{u}{r^2} \right) + (K-1) \frac{\partial^2 u}{\partial z^2} + 2 \frac{\partial^2 w}{\partial r \partial z} &= 0 \\
2 \left( \frac{\partial^2 u}{\partial r \partial z} + \frac{1}{r} \frac{\partial u}{\partial z} \right) + (K-1) \left( \frac{\partial^2 w}{\partial r^2} + \frac{1}{r} \frac{\partial w}{\partial r} \right) + (K+1) \left( \frac{\partial^2 w}{\partial z^2} \right) &= 0
\end{aligned} \tag{2.6a-b}$$

The Navier equations must be solved using the boundary conditions:

$$\begin{aligned}
\sigma_z(r, -\infty) &= 0 & (A < r < B) \\
\sigma_z(r, +\infty) &= 0 & (A < r < B) \\
w(r, 0) &= 0 & (A < r < a), (b < r < B) \\
\sigma_z(r, 0) &= -p(r) & (a < r < b) \\
\sigma_r(A, z) &= 0 & (-\infty < z < \infty) \\
\tau_{rz}(A, z) &= 0 & (-\infty < z < \infty) \\
u(B, z) &= 0 & (-\infty < z < \infty) \\
w(B, z) &= 0 & (-\infty < z < \infty) \\
\tau_{rz}(r, 0) &= 0 & (a < r < b)
\end{aligned} \tag{2.7a-i}$$

where  $p(r)$  is the intensity of the distributed load on the crack surfaces.

### 2.1.1. The Perturbation Problem

The solution for the infinite hollow cylinder containing a ring-shaped crack may be found by the superposition of the solutions for two sub-problems as showed in Figure 2.2: (1) The problem of an infinite elastic medium containing a ring-shaped crack of width  $(b-a)$  at the symmetry plane and (2) the problem of an infinite medium without crack subjected to arbitrary symmetric loads.

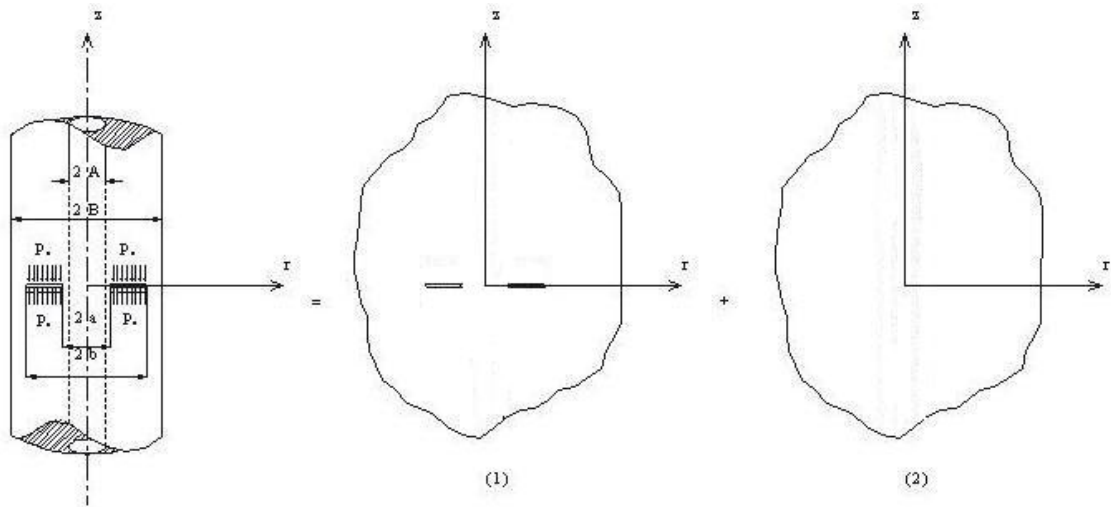


Figure 2.2. Perturbation problem

#### 2.1.1.1. An Infinite Elastic Medium having a Crack

Consider an infinite medium containing a crack at  $z = 0$  plane,  $z$  is the axis of the medium. The crack surfaces are under the action of distributed axisymmetric compressive loads.

Because of the symmetry, it is sufficient to consider one half of the medium ( $z \geq 0$ ) instead of considering both parts of the medium. Displacement and stress components will be obtained by using Hankel transformation technique.

By using Hankel transform definition

$$H_n\{f(ax); \varphi\} = \int_0^\infty f(ax)x J_n(x\varphi) dx \quad (a > 0) \quad (2.8)$$

where  $n = 0$  for even and  $n = 1$  for odd functions.  $u(r, z)$  is an odd and  $w(r, z)$  is an even function in  $r$  direction, Hankel transform of the displacement functions can be written in the form of

$$\begin{aligned} H_1\{u(r, z); \alpha\} &= \int_0^\infty u(r, z) r J_1(r\alpha) dr = U(\alpha, z) \\ H_0\{w(r, z); \alpha\} &= \int_0^\infty w(r, z) r J_0(r\alpha) dr = W(\alpha, z) \end{aligned} \quad (2.9a-b)$$

where  $J_0$  and  $J_1$  are the Bessel functions of the first kind of order zero and one, respectively. Applying Hankel transform to equation (2.6) in  $r$  direction, the following equations can be obtained

$$\begin{aligned} -(K + 1)\alpha^2 U(\alpha, z) + (K - 1) \frac{d^2 U(\alpha, z)}{dz^2} - 2\alpha^2 \frac{dW}{dz} &= 0 \\ 2\alpha \frac{dU}{dz} - (K - 1)\alpha^2 W(\alpha, z) + (K + 1) \frac{d^2 W(\alpha, z)}{dz^2} &= 0 \end{aligned} \quad (2.10a-b)$$

By doing some manipulations, the equation system (2.10) can be reduced to a fourth order ordinary differential equation in the form:

$$\frac{d^4 U(\alpha, z)}{dz^4} - 2\alpha^2 \frac{d^2 U(\alpha, z)}{dz^2} + \alpha^4 U(\alpha, z) = 0 \quad (2.11)$$

The general solution of the equation (2.11) is found as

$$U(\alpha, z) = (c_1 + c_2 z)e^{-\alpha z} + (c_3 + c_4 z)e^{\alpha z} \quad (2.12)$$

where  $c_1, c_2, c_3$  and  $c_4$  are arbitrary unknown constants and  $\alpha > 0$ .

In order to get finite displacement at infinity, constants  $c_3$  and  $c_4$  must be equal to zero for the upper half of the medium ( $z > 0$ ) and constants  $c_1$  and  $c_2$  must be equal to zero for the lower half of the medium ( $z < 0$ ). Therefore, considering subscripts  $u$  and  $l$  indicate the upper and the lower half of the medium respectively, equation (2.12) can be expressed in the form of

$$\begin{aligned}
U_u(\alpha, z) &= (c_1 + c_2 z)e^{-\alpha z} & (z \geq 0) \\
U_l(\alpha, z) &= (c_3 + c_4 z)e^{\alpha z} & (z \leq 0)
\end{aligned} \tag{2.13a-b}$$

Using the same procedure for  $W(\alpha, z)$ , the solutions can be found as

$$\begin{aligned}
W_u(\alpha, z) &= \left[ (c_1 + c_2 z) + \frac{K}{\alpha} c_2 \right] e^{-\alpha z} & (z \geq 0) \\
W_l(\alpha, z) &= \left[ -(c_3 + c_4 z) + \frac{K}{\alpha} c_4 \right] e^{\alpha z} & (z \leq 0)
\end{aligned} \tag{2.14a-b}$$

By taking inverse transforms of equations (2.13a-b) and (2.14a-b), displacement components are found as

$$\begin{aligned}
u_u(r, z) &= \int_0^\infty (c_1 + c_2 z) e^{-\alpha z} \alpha J_1(\alpha r) d\alpha & (z \geq 0) \\
u_l(r, z) &= \int_0^\infty (c_3 + c_4 z) e^{\alpha z} \alpha J_1(\alpha r) d\alpha & (z \leq 0) \\
w_u(r, z) &= \int_0^\infty \left[ (c_1 + c_2 z) + \frac{K}{\alpha} c_2 \right] e^{-\alpha z} \alpha J_0(\alpha r) d\alpha & (z \geq 0) \\
w_l(r, z) &= \int_0^\infty \left[ -(c_3 + c_4 z) + \frac{K}{\alpha} c_4 \right] e^{\alpha z} \alpha J_0(\alpha r) d\alpha & (z \leq 0)
\end{aligned} \tag{2.15a-d}$$

By substituting the equations (2.15a-d) into the expressions given in the equations (2.5a-d), stress components can be found as

$$\begin{aligned}
\sigma_{r_u}(r, z) &= \mu \int_0^\infty [2(c_1 + c_2 z)\alpha - (3 - K)c_2] e^{-\alpha z} \alpha J_0(\alpha r) d\alpha & (z \geq 0) \\
&\quad + \mu \int_0^\infty -2(c_1 + c_2 z) e^{-\alpha z} \frac{\alpha}{r} J_1(\alpha r) d\alpha \\
\sigma_{r_l}(r, z) &= \mu \int_0^\infty [2(c_3 + c_4 z)\alpha + (3 - K)c_4] e^{\alpha z} \alpha J_0(\alpha r) d\alpha & (z \leq 0) \\
&\quad + \mu \int_0^\infty -2(c_3 + c_4 z) e^{\alpha z} \frac{\alpha}{r} J_1(\alpha r) d\alpha \\
\sigma_{z_u}(r, z) &= \mu \int_0^\infty [-(K + 1)c_2 - 2(c_1 + c_2 z)\alpha] e^{-\alpha z} \alpha J_0(\alpha r) d\alpha & (z \geq 0)
\end{aligned}$$

$$\begin{aligned}
\sigma_{z_l}(r, z) &= \mu \int_0^{\infty} [(K+1)c_4 - 2(c_3 + c_4 z)\alpha] e^{\alpha z} \alpha J_0(\alpha r) d\alpha & (z \leq 0) \\
\tau_{rz_u}(r, z) &= \mu \int_0^{\infty} [-(K-1)c_2 - 2(c_1 + c_2 z)\alpha] e^{-\alpha z} \alpha J_1(\alpha r) d\alpha & (z \geq 0) \\
\tau_{rz_l}(r, z) &= \mu \int_0^{\infty} [-(K-1)c_4 + 2(c_3 + c_4 z)\alpha] e^{\alpha z} \alpha J_1(\alpha r) d\alpha & (z \leq 0) \quad (2.16a-f)
\end{aligned}$$

These expressions satisfies the following continuity and symmetry conditions on  $z = 0$  plane.

$$\begin{aligned}
\sigma_{z_u}(r, 0) &= \sigma_{z_l}(r, 0) & 0 \leq r \leq \infty \\
\tau_{z_u}(r, 0) &= \tau_{z_l}(r, 0) & 0 \leq r \leq \infty \\
\frac{\partial}{\partial r} [u_u(r, 0) - u_l(r, 0)] &= 0 & 0 \leq r \leq \infty \\
\frac{\partial}{\partial r} [w_u(r, 0) - w_l(r, 0)] &= 2f(r) & 0 \leq r \leq \infty \quad (2.17a-d)
\end{aligned}$$

where  $f(r)$  is the unknown crack surface displacement derivative such that  $f(r) = 0$  when  $(A \leq r < a, b \leq r < B)$ . Using the conditions (2.17a-d), the unknown constants  $c_1, c_2, c_3$  and  $c_4$  can be found as

$$\begin{aligned}
c_1 = c_3 &= \frac{F(\alpha) (K-1)}{\alpha (K+1)} \\
c_2 = -c_4 &= -\frac{2F(\alpha)}{(K+1)}
\end{aligned} \quad (2.18a-b)$$

where  $F(\alpha) = \int_a^b f(r) r J_1(\alpha r) dr$ .

The hollow cylinder containing a ring-shaped crack is symmetric about  $z$  axis and it is sufficient to consider the solution of the axisymmetric problem in the upper or lower half of the medium. Therefore, the general expressions for the displacement and the stress components in the upper half of the medium are in the form of

$$\begin{aligned}
u_{hankel}(r, z) &= \frac{1}{(K+1)} \int_0^{\infty} [(K-1) - 2\alpha z] F(\alpha) e^{-\alpha z} J_1(\alpha r) d\alpha \\
w_{hankel}(r, z) &= \frac{1}{(K+1)} \int_0^{\infty} [-(K+1) - 2\alpha z] F(\alpha) e^{-\alpha z} J_0(\alpha r) d\alpha \\
\sigma_{rhankel}(r, z) &= \frac{2\mu}{(K+1)} \int_0^{\infty} 2(1 - \alpha z) F(\alpha) e^{-\alpha z} \alpha J_0(\alpha r) d\alpha \\
&\quad + \frac{2\mu}{(K+1)} \int_0^{\infty} 2\alpha z - (K-1) F(\alpha) e^{-\alpha z} \frac{1}{r} J_1(\alpha r) d\alpha \\
\sigma_{zhankel}(r, z) &= \frac{4\mu}{(K+1)} \int_0^{\infty} (1 + \alpha z) F(\alpha) e^{-\alpha z} \alpha J_0(\alpha r) d\alpha \\
\tau_{rzhankel}(r, z) &= \frac{4\mu}{(K+1)} \int_0^{\infty} \alpha z F(\alpha) \alpha e^{-\alpha z} J_1(\alpha r) d\alpha \tag{2.19a-e}
\end{aligned}$$

### 2.1.1.2. An Infinite Elastic Medium without a Crack

An infinite elastic medium without a crack that is loaded symmetrically is considered. This infinite elastic medium is symmetric about z-axis and  $z = 0$  plane. The Fourier transforms of the displacement components are written below using the Fourier sine and cosine transform definitions:

$$\begin{aligned}
F_c\{u(r, z); \lambda\} &= \frac{2}{\pi} \int_0^{\infty} u(r, z) \cos(\lambda r) dr = U(r, \lambda) \\
F_s\{w(r, z); \lambda\} &= \frac{2}{\pi} \int_0^{\infty} w(r, z) \cos(\lambda r) dr = W(r, \lambda) \tag{2.20a-b}
\end{aligned}$$

where  $U(r, \lambda)$  and  $W(r, \lambda)$  are the Fourier cosine and sine transforms of functions  $u(r, z)$  and  $w(r, z)$ , respectively,  $\lambda$  is the Fourier transform variable. Noting that  $u(r, z)$  is even and  $w(r, z)$  is odd functions in  $z$ , the Fourier cosine and sine transforms may be applied to equation (2.6a-b) and the system of second order ordinary differential equation is obtained as

$$\begin{aligned}
(K+1) \left[ \frac{d^2 U}{dr^2} + \frac{1}{r} \frac{dy}{dx} - \frac{U}{r} \right] - (K-1) \lambda^2 U + 2\lambda \frac{dW}{dr} &= 0 \\
-2\lambda \frac{dU}{dr} - \frac{2}{r} \lambda U + (K-1) \left[ \frac{d^2 W}{dr^2} + \frac{1}{r} \frac{dW}{dr} \right] - (K+1) \lambda^2 W &= 0
\end{aligned} \quad (2.21a-b)$$

Equations (2.21a-b) can be reduced to a single equation.

$$\begin{aligned}
r^4 \frac{d^4 U}{dr^4} + 2r^3 \frac{d^3 U}{dr^3} - (2\lambda^2 r^4 + 3r^2) \frac{dy}{dx} - (2\lambda^2 r^3 - 3r) \frac{dy}{dx} \\
+ (\lambda^4 r^4 + 2\lambda^2 r^2 - 3)U = 0
\end{aligned} \quad (2.22)$$

The solution of this reduced equation can be found in a previous study of (Artem and Geçit 2002) as

$$\begin{aligned}
U(r, \lambda) &= -\frac{1}{2} c_5 I_1(\lambda r) + \frac{1}{2} c_6 K_1(\lambda r) + c_7 \lambda r I_0(\lambda r) + c_8 \lambda r K_0(\lambda r) \\
W(r, \lambda) &= \frac{1}{2} c_5 I_0(\lambda r) + \frac{1}{2} c_6 K_0(\lambda r) - c_7 [(K+1)I_0(\lambda r) + \lambda r I_1(\lambda r)] \\
&\quad - c_8 [(K+1)K_0(\lambda r) - \lambda r K_1(\lambda r)]
\end{aligned} \quad (2.23a-b)$$

where  $c_5, c_6, c_7$  and  $c_8$  are arbitrary constants,  $I_0$  and  $I_1$  are the modified Bessel functions of the first kind of order zero and one, respectively,  $K_0$  and  $K_1$  are the modified Bessel functions of the second kind of order zero and one, respectively.

By taking inverse Fourier cosine and sine transforms of equations (2.23a-b), the displacement components can be expressed as

$$\begin{aligned}
u(r, z)_{fourier} &= \frac{2}{\pi} \int_0^\infty \left[ -\frac{1}{2} c_5 I_1(\lambda r) + \frac{1}{2} c_6 K_1(\lambda r) + c_7 \lambda r I_0(\lambda r) \right. \\
&\quad \left. + c_8 \lambda r K_0(\lambda r) \right] \cos \lambda z d\lambda \\
w(r, z)_{fourier} &= \frac{2}{\pi} \int_0^\infty \left\{ \frac{1}{2} c_5 I_0(\lambda r) + \frac{1}{2} c_6 K_0(\lambda r) \right. \\
&\quad - c_7 [(K+1)I_0(\lambda r) + \lambda r I_1(\lambda r)] \\
&\quad \left. - c_8 [(K+1)K_0(\lambda r) - \lambda r K_1(\lambda r)] \right\} \sin \lambda z d\lambda
\end{aligned} \quad (2.24a-b)$$



And the stress components can be found by substituting equations (2.24a-b) into stress-displacement relations equation (2.5a-d).

$$\begin{aligned}
\sigma_r(r, z)_{fourier} &= \frac{2\mu}{\pi} \int_0^\infty \left\{ c_5 \left[ -\lambda I_0(\lambda r) + \frac{1}{r} I_1(\lambda r) \right] + c_6 \left[ -\lambda K_0(\lambda r) - \right. \right. \\
&\quad \left. \left. \frac{1}{r} K_1(\lambda r) \right] + c_7 [(K-1)\lambda I_0(\lambda r) + 2\lambda^2 r I_1(\lambda r)] + \right. \\
&\quad \left. c_8 [(K-1)\lambda K_0(\lambda r) - 2\lambda^2 r K_1(\lambda r)] \right\} \cos \lambda z d\lambda \\
\sigma_z(r, z)_{fourier} &= \frac{2\mu}{\pi} \int_0^\infty \left\{ c_5 \lambda I_0(\lambda r) + c_6 \lambda K_0(\lambda r) - c_7 [(K+ \right. \\
&\quad \left. 5)\lambda I_0(\lambda r) + 2\lambda^2 r I_1(\lambda r)] - c_8 [(K+5)\lambda K_0(\lambda r) - \right. \\
&\quad \left. 2\lambda^2 r K_1(\lambda r)] \right\} \cos \lambda z d\lambda \\
\tau_{rz}(r, z)_{fourier} &= \frac{2\mu}{\pi} \int_0^\infty \left\{ c_5 \lambda I_1(\lambda r) - c_6 \lambda K_1(\lambda r) - c_7 [(K+ \right. \\
&\quad \left. 1)\lambda I_1(\lambda r) + 2\lambda^2 r I_0(\lambda r)] - c_8 [(K+1)\lambda K_1(\lambda r) - \right. \\
&\quad \left. 2\lambda^2 r K_0(\lambda r)] \right\} \cos \lambda z d\lambda
\end{aligned} \tag{2.25a-c}$$

### 2.1.2. General Solution

The general solution of the problem can be found by adding the expressions for the displacement and the stress components found in the problem of an infinite elastic medium having a crack (Hankel Transformation) and the problem of an infinite elastic medium without a crack (Fourier Transformation).

$$\begin{aligned}
u(r, z) &= u(r, z)_{hankel} + u(r, z)_{fourier} \\
w(r, z) &= w(r, z)_{hankel} + w(r, z)_{fourier} \\
\sigma_z(r, z) &= \sigma_z(r, z)_{hankel} + \sigma_z(r, z)_{fourier} \\
\sigma_r(r, z) &= \sigma_r(r, z)_{hankel} + \sigma_r(r, z)_{fourier} \\
\tau_{rz}(r, z) &= \tau_{rz}(r, z)_{hankel} + \tau_{rz}(r, z)_{fourier}
\end{aligned} \tag{2.26a-e}$$

The arbitrary unknown constants  $c_5, c_6, c_7$  and  $c_8$  can be written in the terms of unknown function  $F(\alpha)$  with the conditions given for inner and outer lateral surfaces of the cylinder:

$$\begin{aligned}
u(B, z) &= 0 \\
w(B, z) &= 0 \\
\sigma_r(A, z) &= 0 \\
\tau_{rz}(A, z) &= 0
\end{aligned} \tag{2.27a-d}$$

Therefore, a system of equations can be obtained by applying the boundary conditions given for inner and outer surfaces of the cylinder to the equations (2.19a-e), (2.24a-b) and (2.25a-c):

$$\begin{aligned}
& -\frac{1}{2}c_5I_1(\lambda B) + \frac{1}{2}c_6K_1(\lambda B) + c_7\lambda BI_0(\lambda B) + c_8\lambda BK_0(\lambda B) \\
& \quad = -\frac{1}{(K+1)}\int_0^\infty \left\{ \int_0^\infty [(K-1) - 2\alpha z]F(\alpha)e^{-\alpha z}J_1(\alpha B) d\alpha \right\} \cos \lambda z dz \\
& \frac{1}{2}c_5I_0(\lambda B) + \frac{1}{2}c_6K_0(\lambda B) - c_7[(K+1)I_0(\lambda B) + \lambda BI_1(\lambda B)] \\
& \quad - c_8[(K+1)K_0(\lambda B) - \lambda rK_1(\lambda B)] \\
& \quad = -\frac{1}{(K+1)}\int_0^\infty \left\{ \int_0^\infty [-(K+1) - 2\alpha z]F(\alpha)e^{-\alpha z}J_0(\alpha B) d\alpha \right\} \sin \lambda z dz \\
& c_5 \left[ -\lambda I_0(\lambda A) + \frac{1}{A}I_1(\lambda A) \right] + c_6 \left[ -\lambda K_0(\lambda A) - \frac{1}{A}K_1(\lambda A) \right] \\
& \quad + c_7[(K-1)\lambda I_0(\lambda A) + 2\lambda^2 AI_1(\lambda A)] \\
& \quad + c_8[(K-1)\lambda K_0(\lambda A) - 2\lambda^2 AK_1(\lambda A)] \\
& \quad = -\frac{2}{(K+1)}\int_0^\infty \left\{ \int_0^\infty \left\{ [2\alpha z - (K-1)]\frac{1}{r}J_1(\alpha A) \right. \right. \\
& \quad \left. \left. + 2(1-\alpha z)\alpha J_0(\alpha A) \right\} F(\alpha)e^{-\alpha z} d\alpha \right\} \cos \lambda z dz \\
& c_5\lambda I_1(\lambda A) - c_6\lambda K_1(\lambda A) - c_7[(K+1)\lambda I_1(\lambda A) + 2\lambda^2 AI_0(\lambda A)] \\
& \quad - c_8[(K+1)\lambda K_1(\lambda A) - 2\lambda^2 AK_0(\lambda A)] \\
& \quad = -\frac{4}{(K+1)}\int_0^\infty \left\{ \int_0^\infty \alpha z F(\alpha) \alpha e^{-\alpha z} J_1(\alpha A) d\alpha \right\} \sin \lambda z dz
\end{aligned} \tag{2.28a-d}$$

This system of equations (2.28a-d) is in double integral form and it can be reduced to a single integral form by using the integral formulas given in Appendix A.

$$\begin{aligned}
& -\frac{1}{2}c_5I_1(\lambda B) + \frac{1}{2}c_6K_1(\lambda B) + c_7\lambda BI_0(\lambda B) + c_8\lambda BK_0(\lambda B) \\
& = -\frac{1}{(K+1)}\int_a^b f(t)t[(K+1)I_1(t\lambda)K_1(B\lambda) + 2\lambda BI_1(t\lambda)K_0(B\lambda) \\
& \quad - 2\lambda tI_0(t\lambda)K_1(B\lambda)] dt \\
& \frac{1}{2}c_5I_0(\lambda B) + \frac{1}{2}c_6K_0(\lambda B) - c_7[(K+1)I_0(\lambda B) + \lambda BI_1(\lambda B)] \\
& \quad - c_8[(K+1)K_0(\lambda B) - \lambda rK_1(\lambda B)] \\
& = -\frac{1}{(K+1)}\int_a^b f(t)t[-2t\lambda I_0(t\lambda)K_0(B\lambda) - (K+1)I_1(t\lambda)K_0(B\lambda) \\
& \quad + 2B\lambda I_1(t\lambda)K_1(B\lambda)] dt \\
& c_5\left[-\lambda I_0(\lambda A) + \frac{1}{A}I_1(\lambda A)\right] + c_6\left[-\lambda K_0(\lambda A) - \frac{1}{A}K_1(\lambda A)\right] \\
& \quad + c_7[(K-1)\lambda I_0(\lambda A) + 2\lambda^2 AI_1(\lambda A)] \\
& \quad + c_8[(K-1)\lambda K_0(\lambda A) - 2\lambda^2 AK_1(\lambda A)] \\
& = -\frac{1}{(K+1)}\int_a^b f(t)t\left[-4(tI_0(A\lambda)K_0(t\lambda) - AI_1(A\lambda)K_1(t\lambda))\lambda^2 \right. \\
& \quad \left. + \frac{4(tI_1(A\lambda)K_0(t\lambda) - AI_1(A\lambda)K_0(t\lambda))\lambda}{A} + \frac{2(K+1)I_1(A\lambda)K_1(t\lambda)}{A}\right] dt \\
& c_5\lambda I_1(\lambda A) - c_6\lambda K_1(\lambda A) - c_7[(K+1)\lambda I_1(\lambda A) + 2\lambda^2 AI_0(\lambda A)] \\
& \quad - c_8[(K+1)\lambda K_1(\lambda A) - 2\lambda^2 AK_0(\lambda A)] \\
& = -\frac{1}{(K+1)}\int_a^b f(t)t\left[\frac{1}{2}\lambda^2(AI_0(A\lambda)K_1(t\lambda) \right. \\
& \quad \left. - tI_1(A\lambda)K_0(t\lambda))\right] dt \tag{2.29a-d}
\end{aligned}$$

Equation (2.29a-d) can now be rewritten as

$$\begin{aligned}
-\frac{1}{2}c_5I_1(\lambda B) + \frac{1}{2}c_6K_1(\lambda B) + c_7\lambda BI_0(\lambda B) + c_8\lambda BK_0(\lambda B) &= E_1 \\
\frac{1}{2}c_5I_0(\lambda B) + \frac{1}{2}c_6K_0(\lambda B) - c_7[(K+1)I_0(\lambda B) + \lambda BI_1(\lambda B)] \\
&\quad - c_8[(K+1)K_0(\lambda B) - \lambda rK_1(\lambda B)] = E_2 \\
c_5\left[-\lambda I_0(\lambda A) + \frac{1}{A}I_1(\lambda A)\right] + c_6\left[-\lambda K_0(\lambda A) - \frac{1}{A}K_1(\lambda A)\right] \\
&\quad + c_7[(K-1)\lambda I_0(\lambda A) + 2\lambda^2 AI_1(\lambda A)] \\
&\quad + c_8[(K-1)\lambda K_0(\lambda A) - 2\lambda^2 AK_1(\lambda A)] = E_3 \\
c_5\lambda I_1(\lambda A) - c_6\lambda K_1(\lambda A) - c_7[(K+1)\lambda I_1(\lambda A) + 2\lambda^2 AI_0(\lambda A)] \\
&\quad - c_8[(K+1)\lambda K_1(\lambda A) - 2\lambda^2 AK_0(\lambda A)] = E_4 \tag{2.30a-d}
\end{aligned}$$

where  $E_1, E_2, E_3$  and  $E_4$  are given in Appendix B and  $c_5, c_6, c_7$  and  $c_8$  are unknown constants. Now  $c_5, c_6, c_7$  and  $c_8$  can be found in terms of  $E_1, E_2, E_3$  and  $E_4$  by solving this system of equations (Equations (2.30)) :

$$\begin{aligned}
c_5 &= \frac{(l_{11}E_1 + l_{12}E_2 + l_{13}E_3 + l_{14}E_4)}{P} \\
c_6 &= \frac{(l_{21}E_1 + l_{22}E_2 + l_{23}E_3 + l_{24}E_4)}{P} \\
c_7 &= \frac{(l_{31}E_1 + l_{32}E_2 + l_{33}E_3 + l_{34}E_4)}{P} \\
c_8 &= \frac{(l_{41}E_1 + l_{42}E_2 + l_{43}E_3 + l_{44}E_4)}{P} \tag{2.31a-d}
\end{aligned}$$

where  $l_{11} - l_{44}$  and  $P$  are given in Appendix B.

The expressions for  $c_5, c_6, c_7$  and  $c_8$  are found by using the boundary conditions on the lateral surfaces of the cylinder. The unknown function  $F(\alpha)$  can be found by using the remaining boundary condition that is  $\sigma_z(r, 0) = -p(r)$  on the crack surfaces.

## CHAPTER 3

### INTEGRAL EQUATION

#### 3.1. Derivation of Integral Equation

The expression for  $\sigma_z(r, z)$  can be obtained in terms of the unknown function  $F(\alpha)$  by substituting equation (2.19d) and equation (2.25b) into the equation (2.26c).

$$\begin{aligned} \sigma_z(r, z) = & \frac{4\mu}{(K+1)} \int_0^\infty (\alpha z + 1) F(\alpha) e^{-\alpha z} \alpha J_0(\alpha r) d\alpha \\ & + \frac{2\mu}{\pi} \int_0^\infty [c_5 \lambda I_0(\lambda r) + c_6 \lambda K_0(\lambda r) \\ & - c_7 [(K+5)\lambda I_0(\lambda r) + 2\lambda^2 r I_1(\lambda r)] \\ & - c_8 [(K+5)\lambda K_0(\lambda r) - 2\lambda^2 r K_1(\lambda r)]] \cos \lambda z d\lambda \end{aligned} \quad (3.1)$$

The remaining boundary condition  $\sigma_z(r, 0) = -p(r)$  can be applied now

$$\begin{aligned} \sigma_z(r, 0) = & \frac{4\mu}{(K+1)} \int_0^\infty F(\alpha) \alpha J_0(\alpha r) d\alpha \\ & + \frac{2\mu}{\pi} \int_0^\infty [c_5 \lambda I_0(\lambda r) + c_6 \lambda K_0(\lambda r) \\ & - c_7 [(K+5)\lambda I_0(\lambda r) + 2\lambda^2 r I_1(\lambda r)] \\ & - c_8 [(K+5)\lambda K_0(\lambda r) - 2\lambda^2 r K_1(\lambda r)]] d\lambda = -p(r) \end{aligned} \quad (3.2)$$

Equation (3.2) can be reduced to a singular integral equation with kernel having Cauchy type singularity (Muskhelishvili 1953):

$$\frac{2\mu}{\pi(K+1)} \int_a^b f(t) \left[ \frac{2}{t-r} + 2M_1(r, t) + tS_{11}(r, t) \right] dt = -p(r) \quad (a < r < b) \quad (3.3)$$

where

$$M_1(r, t) = \frac{M_1^*(r, t) - 1}{t - r} \quad (r > t) \quad (3.4)$$

$$M_1^*(r, t) = \begin{cases} \frac{2(t-r)}{r} K\left(\frac{t}{r}\right) + \frac{2r}{t+r} E\left(\frac{t}{r}\right), & r > t \\ \frac{2t}{t+r} E\left(\frac{r}{t}\right), & r < t \end{cases} \quad (3.5)$$

$K$  and  $E$  are the complete elliptic integrals of the first and the second kinds, respectively. The equation (3.3) must be solved under the condition for the displacement around the crack given as

$$\int_a^b f(t) dt = 0 \quad (3.6)$$

The integral equation (3.3) has three types of singularities

- Cauchy type singularity at  $t = r$
- Logarithmic singularity in the kernel  $M_1(r, t)$
- The integral  $S_{11}(r, t)$  has singular terms at  $t = A$ ,  $t = B$  and  $r = \pm A$ ,  $r = \pm B$  because of the integrand behaviour as  $\lambda \rightarrow \infty$ .

The integral  $S_{11}(r, t)$  can be rewritten as

$$S_{11}(r, t) = S_{11s}(r, t) + S_{11b}(r, t) \quad (3.7)$$

where  $S_{11s}(r, t)$  and  $S_{11b}(r, t)$  denotes singular and bounded part of the integrand respectively. Then  $S_{11}(r, t)$  can be expressed as

$$S_{11}(r, t) = \int_0^\infty N_{11}(r, t, \lambda) d\lambda \quad (3.8)$$

The singular part of  $S_{11}(r, t)$  can be separated as

$$S_{11s}(r, t) = \int_0^\infty N_{11s}(r, t, \lambda) d\lambda \quad (3.9)$$

The integrand of the equation (3.9) has the modified Bessel functions  $I_0, K_0, I_1$  and  $K_1$ . Applying the asymptotic expansions for the modified Bessel functions are given in the Appendix C and by doing some manipulations the integrand of the singular part of the integral  $S_{11}(r, t)$  can be found as

$$\begin{aligned}
N_{11s}(r, t, \lambda) = & \frac{1}{\sqrt{rt}} \left\{ e^{-\lambda(2B-r-t)} \left[ \frac{1}{K} (-4(B-r)(B-t)\lambda^2 - 2(B-r)\lambda \right. \right. \\
& + 6(B-t)\lambda + (K^2 + 3)) \Big] \\
& + e^{\lambda(2A-r-t)} [4(A-r)(A-t)\lambda^2 + 2(A-r)\lambda + 6(A-t)\lambda \\
& \left. \left. + 4] \right\} \tag{3.10}
\end{aligned}$$

The integrand of the singular part of the integral  $S_{11}(r, t)$  can be obtained by using the integration formula given in Appendix D as

$$\begin{aligned}
N_{11s}(r, t, \lambda) = & \frac{1}{\sqrt{rt}} \left\{ \left[ \frac{1}{K} \left( -4(B-r)^2 \frac{d^2}{dr^2} - 12(B-r) \frac{d}{dr} \right. \right. \right. \\
& \left. \left. \left. + (-K^2 + 3) \right) \right] \frac{1}{t - (2B - r)} \right. \\
& \left. + \left[ -4(A-r)^2 \frac{d^2}{dr^2} + 12(A-r) \frac{d}{dr} - 2 \right] \frac{1}{t - (2A - r)} \right\} \tag{3.11}
\end{aligned}$$

Therefore, the bounded part of the integral  $S_{11}(r, t)$  can be found as

$$S_{11b}(r, t) = \int_0^\infty [N_{11}(r, t, \lambda) - N_{11s}(r, t, \lambda)] d\lambda \tag{3.12}$$

The equation (3.3) can now be rewritten as

$$\frac{1}{\pi} \int_a^b f(t) \left[ \frac{2}{t-r} + tS_{11}(r, t) \right] dt = B(r) \quad (a < r < b) \tag{3.13}$$

where  $B(r)$  is the function that contains all the bounded terms of the equation (3.3).

### 3.2. Characteristic Equation

The unknown function  $f(t)$  is expected to have integrable singularities at the tips of the crack. Therefore, the singular behaviour of the unknown function  $f(t)$  can be determined by writing

$$f(t) = \frac{F^*(t)}{(t-a)^\beta(b-t)^\gamma} \quad \begin{array}{l} (0 < \operatorname{Re}(\gamma) < 1) \\ (0 < \operatorname{Re}(\beta) < 1) \end{array} \quad (3.14)$$

where  $F^*(t)$  is Hölder continuous function (Muskhelishvili 1953) in the interval  $[a, b]$ ,  $\gamma$  and  $\beta$  are the unknown constants. The unknown constants  $\gamma$  and  $\beta$  can be found by examining the integral equation (3.13) near the ends  $r = a$  and  $r = b$ .

The integral equation (3.13), together with equation (3.14) can be written as

$$\frac{1}{\pi} \int_a^b \frac{F^*(t)}{(t-a)^\beta(b-t)^\gamma} \left[ \frac{2}{t-r} + tS_{11}(r, t) \right] dt = B(r) \quad (a < r < b) \quad (3.15)$$

The integral on the left-hand side of the equation (3.15) near the ends  $r = a$  and  $r = b$  can be calculated with the help of the complex function technique described in (Muskhelishvili 1953). The required integrals are

$$\begin{aligned} \frac{1}{\pi} \int_a^b \frac{f(t)}{(t-r)} dt &= \frac{F^*(a) \cot \pi\gamma}{(b-a)^\gamma(r-a)^\beta} - \frac{F^*(b) \cot \pi\gamma}{(b-a)^\beta(b-r)^\gamma} + L(r) \\ \frac{1}{\pi} \int_A^B \frac{f(t)}{(t-(2A-r))} dt &= \frac{F^*(A)e^{\pi\beta i}}{(B-A)^\gamma((2A-r)-A)^\beta \sin \pi\beta} \\ &\quad - \frac{F^*(B)e^{-\pi\gamma i}}{(B-A)^\beta(B-(2A-r))^\gamma \sin \pi\gamma} + A_1(r) \end{aligned}$$



$$\begin{aligned}
& \frac{d}{dr} \frac{1}{\pi} \int_A^B \frac{f(t)}{(t - (2A - r))} dt \\
&= \frac{F^*(A)e^{\pi\beta i} \beta}{(B - A)^\gamma (A - r)^{\beta+1} \sin \pi\beta} - \frac{F^*(B)e^{-\pi\gamma i} \gamma}{(B - A)^\beta (B - (2A - r))^{\gamma+1} \sin \pi\gamma} \\
&+ A_2(r) \\
& \frac{d^2}{dr^2} \frac{1}{\pi} \int_A^B \frac{f(t)}{(t - (2A - r))} dt \\
&= \frac{F^*(A)e^{\pi\beta i} \beta(\beta + 1)}{(B - A)^\gamma (A - r)^{\beta+2} \sin \pi\beta} - \frac{F^*(B)e^{-\pi\gamma i} \gamma(\gamma + 1)}{(B - A)^\beta (B - (2A - r))^{\gamma+2} \sin \pi\gamma} \\
&+ A_3(r) \\
& \frac{1}{\pi} \int_A^B \frac{f(t)}{(t - (2B - r))} dt \\
&= \frac{F^*(A)e^{\pi\beta i}}{(B - A)^\gamma ((2B - r) - A)^\beta \sin \pi\beta} \\
&- \frac{F^*(B)e^{-\pi\gamma i}}{(B - A)^\beta (B - (2B - r))^\gamma \sin \pi\gamma} + B_1(r) \\
& \frac{d}{dr} \frac{1}{\pi} \int_A^B \frac{f(t)}{(t - (2B - r))} dt \\
&= \frac{F^*(A)e^{\pi\beta i} \beta}{(B - A)^\gamma ((2B - r) - A)^{\beta+1} \sin \pi\beta} - \frac{F^*(B)e^{-\pi\gamma i} \gamma}{(B - A)^\beta (r - B)^{\gamma+1} \sin \pi\gamma} \\
&+ B_2(r) \\
& \frac{d^2}{dr^2} \frac{1}{\pi} \int_A^B \frac{f(t)}{(t - (2B - r))} dt \\
&= \frac{F^*(A)e^{\pi\beta i} \beta(\beta + 1)}{(B - A)^\gamma ((2B - r) - A)^{\beta+2} \sin \pi\beta} \\
&- \frac{F^*(B)e^{-\pi\gamma i} \gamma(\gamma + 1)}{(B - A)^\beta (r - B)^{\gamma+2} \sin \pi\gamma} + B_3(r)
\end{aligned} \tag{3.16a-g}$$

where  $L(r)$ ,  $A_{1-3}(r)$  and  $B_{1-3}(r)$  are the bounded parts.

### 3.2.1 Internal Crack

By substituting the equation (3.16a) into the equation (3.15) and multiplying the resulting equation by  $(r - a)^\beta$  and considering the limiting case  $r \rightarrow a$  for an internal crack ( $A < a$ ), the following characteristic equation for  $\beta$  can be obtained as

$$\cos \pi\beta = 0 \quad (3.17)$$

Therefore,  $\beta = \frac{1}{2}$  that is in perfect agreement with the results for an embedded crack tip in a homogeneous medium.

By substituting the equation (3.16a) into the equation (3.15) and multiplying the resulting equation by  $(r - b)^\gamma$  and considering the limiting case  $r \rightarrow b$  for an internal crack ( $b < B$ ), the following characteristic equation for  $\gamma$  can be obtained as

$$\cos \pi\gamma = 0 \quad (3.18)$$

Therefore,  $\gamma = \frac{1}{2}$  is obtained for this case.

These results are in agreement with the previous studies, (Cook ve Erdoğan 1972), (Gupta 1974), (Delale ve Erdoğan 1982), (Nied ve F. 1983), (Artem ve Geçit 2002), (Aydın ve Artem 2007).

### 3.2.2 Crack Terminating at Rigid Surface

When the crack spreads out at the rigid surface along the crack ( $b = A$ ), in addition to equation (3.16a), equation (3.16e-g) must also be substituted into the equation (3.15). Multiplying the resulting equation by  $(B - r)^\gamma$  and considering the limiting case  $r \rightarrow B$ , the following characteristic equation can be obtained as

$$2K \cos \pi\gamma + 4\gamma^2 - 8\gamma + 3 - K^2 = 0 \quad (3.20)$$

The equation (3.20) is in agreement with (Kaman and Gecit 2006).

### 3.2.3 Internal Edge Crack

When the crack spreads out and the cylinder is completely broken along the crack ( $a = A$ ), in addition to equation (3.16a), equation (3.16b-d) must also be substituted into the equation (3.15). Multiplying the resulting equation by  $(A - r)^\beta$  and considering the limiting case  $r \rightarrow A$ , the following characteristic equation for  $\beta$  can be obtained as

$$\cos \pi\beta = 2\beta(\beta - 2) + 1 \quad (3.19)$$

Therefore,  $\beta = 0$  is obtained.

### 3.3. Solution of the Integral Equation

After obtaining the singular behaviour of the unknown function, the integral in the equation (3.3) can be rewritten as a non-dimensional equation by using the dimensionless variables  $\tau$  and  $\xi$  for the cracks:

$$\begin{aligned} t &= \frac{b-a}{2}\tau + \frac{b+a}{2} & (a < t < b), (-1 < \tau < 1) \\ r &= \frac{b-a}{2}\xi + \frac{b+a}{2} & (a < r < b), (-1 < \xi < 1) \end{aligned} \quad (3.21a-b)$$

in the following form

$$\frac{1}{\pi} \int_{-1}^1 \bar{f}(\tau) \left[ \frac{2}{\tau - \xi} + \widehat{M}_1(\xi, \tau) + \widehat{S}_{11}(\xi, \tau) \right] d\tau = -\frac{\bar{p}(\xi)(K+1)}{2\mu} \quad (-1 < \xi < 1) \quad (3.22)$$

where

$$\bar{f}(\tau) = f\left(\frac{b-a}{2}\tau + \frac{b+a}{2}\right) \quad (3.23)$$

$$\widehat{M}_1(\xi, \tau) = (b-a)M_1(\xi, \tau) \quad (3.24)$$

$$\widehat{S}_{11}(\xi, \tau) = \left(\frac{b-a}{2}\right) \left(\frac{b-a}{2}\tau + \frac{b+a}{2}\right) S_{11}(\xi, \tau) \quad (3.25)$$

### 3.3.1 Internal Crack

The singular behaviour of the dimensionless unknown is to be

$$\bar{f}(\tau) = \frac{\overline{F^*}(\tau)}{\sqrt{(1-\tau^2)}} \quad (3.26)$$

where

$$\overline{F^*}(\tau) = F \left( \frac{b-a}{2}\tau + \frac{b+a}{2} \right) \left( \frac{b-a}{2} \right)^{-1} \quad (3.27)$$

Substituting equation (3.26) into the equation (3.22), the following singular integral equation is obtained:

$$\begin{aligned} \frac{1}{\pi} \int_{-1}^1 \frac{\overline{F^*}(\tau)}{\sqrt{(1-\tau^2)}} \left[ \frac{2}{\tau-\xi} + \widehat{M}_1(\xi, \tau) + \widehat{S}_{11}(\xi, \tau) \right] d\tau \\ = - \frac{p(\xi)(K+1)}{2\mu} \end{aligned} \quad (-1 < \xi < 1) \quad (3.28)$$

The integral equation (3.28) can be reduced to an algebraic system by using the Gauss-Lobatto integration formula given in Appendix E:

$$\sum_{i=1}^n C_i \overline{F^*}(\tau_i) \left[ \frac{2}{\tau_i - \xi_j} + \widehat{M}_1(\xi_j, \tau_i) + \widehat{S}_{11}(\xi_j, \tau_i) \right] = - \frac{p(\xi_j)(K+1)}{2\mu} \quad (3.29)$$

where

$$\tau_i = \cos \left[ \frac{(i-1)\pi}{(n-1)} \right] \quad (i = 1, 2, 3, \dots, n) \quad (3.30 \text{ a})$$

$$\xi_j = \cos \left[ \frac{(2j-1)\pi}{2(n-1)} \right] \quad (j = 1, 2, 3, \dots, n-1) \quad (3.30 \text{ b})$$

are the roots of the weighting constants of related Lobatto polynomials. The algebraic system (3.29) has  $n$  unknowns,  $\bar{F}^*(\tau_i)$  and  $(n - 1)$  equations. The single valued condition (Equation (3.6)) must be used to have  $n$  equations because the number of unknowns is larger than the number of the equations. The equation (3.6) becomes

$$\sum_{i=1}^n C_i \bar{F}^*(\tau_i) = 0 \quad (-1 < \tau < 1) \quad (3.31)$$

### 3.3.2 Crack Terminating at Rigid Surface

The singular behaviour of the dimensionless unknown is to be

$$\bar{f}(\tau) = \frac{\bar{F}^*(\tau)}{\sqrt{1 + \tau(1 - \tau)}^\gamma} \quad (3.32)$$

where

$$\bar{F}^*(\tau) = F \left( \frac{b - a}{2} \tau + \frac{b + a}{2} \right) \left( \frac{b - a}{2} \right)^{\frac{1}{2} - \gamma} \quad (3.33)$$

Substituting equation (3.32) into the equation (3.22), the following singular integral equation is obtained:

$$\begin{aligned} \frac{1}{\pi} \int_{-1}^1 \frac{\bar{F}^*(\tau)}{\sqrt{1 + \tau(1 - \tau)}^\gamma} \left[ \frac{2}{\tau - \xi} + \hat{M}_1(\xi, \tau) + \hat{S}_{11}(\xi, \tau) \right] d\tau \\ = - \frac{p(\xi)(K + 1)}{2\mu} \end{aligned} \quad (-1 < \xi < 1) \quad (3.34)$$

The integral equation (3.34) can be reduced to an algebraic system by using the Gauss-Jacobi integration (Erdoğan, et al. 1973):

$$\sum_{i=1}^n W_i \overline{F^*}(\tau_i) \left[ \frac{2}{\tau_i - \xi_j} + \widehat{M}_1(\xi_j, \tau_i) + \widehat{S}_{11}(\xi_j, \tau_i) \right] = -\frac{p(\xi_j)(K+1)}{2\mu} \quad (3.35)$$

where  $W_i$  are the weights,  $\tau_i$  and  $\xi_j$  are the roots of Jacobi polynomials:

$$\begin{aligned} P_n^{(-\alpha, -\beta)}(\tau_i) &= 0 & (i = 1, 2, 3, \dots, n) \\ P_{n-1}^{(1-\alpha, 1-\beta)}(\xi_j) &= 0 & (j = 1, 2, 3, \dots, n-1) \end{aligned} \quad (3.36a-c)$$

The algebraic system (3.35) has  $n$  unknowns,  $\overline{F^*}(\tau_i)$  and  $(n-1)$  equations. The single valued condition (Equation (3.6)) must be used to have  $n$  equations because the number of unknowns is larger than the number of the equations. The equation (3.6) becomes

$$\sum_{i=1}^n W_i \overline{F^*}(\tau_i) = 0 \quad (-1 < \tau < 1) \quad (3.37)$$

The infinite integral appearing in the bounded part of  $\widehat{S}_{11}(\xi, \tau)$  can be obtained numerically by using Laguerre integration method, Appendix E, for each  $\tau_i$  and  $\xi_j$  values. The behaviour of the unknown function at the tips of the crack ( $\tau_i = \pm 1$ ) is characterized by the *stress intensity factor*.

### 3.4. Stress Intensity Factors

The stresses become infinite at the tips of the crack in crack problems. The stress state at close vicinity of the tips of the crack will be presented by the *stress intensity factor*. The stress intensity factors at the tips of the crack will be calculated in the following section.

#### 3.4.1. Stress Intensity Factors at the Tips of Internal Crack

In this study, only Mode I stress intensity factor calculations and investigation will be considered. Mode I stress intensity factor at the tips of the crack has been defined in (Erdol ve Erdođan 1978) as

$$\begin{aligned}
k_1(a) &= \lim_{r \rightarrow a} \sqrt{2(a-r)} \sigma_z(r, 0), \\
k_1(b) &= \lim_{r \rightarrow b} \sqrt{2(r-b)} \sigma_z(r, 0).
\end{aligned} \tag{3.38a-b}$$

$\sigma_z(r, 0)$  can be expressed in terms of the integral equation(3.3):

$$\sigma_z(r, 0) = \frac{4\mu}{\pi(K+1)} \int_a^b \frac{f(t)}{(t-r)} dt + \sigma_{z \text{ bounded}}(r, 0) \tag{3.39}$$

where

$$\sigma_{z \text{ bounded}}(r, 0) = \frac{2\mu}{\pi(K+1)} \int_a^b f(t) [2M_1(r, t) + tS_{11}(r, t)] dt. \tag{3.40}$$

Now  $f(t)$  can be written as

$$f(t) = \frac{F^*(t)}{\sqrt{(t-a)(t-b)}} = \begin{cases} \frac{F^*(t)/\sqrt{(b-t)}}{\sqrt{(t-a)}}, & \text{near } t = a \\ \frac{F^*(t)e^{i\pi/2}/\sqrt{(t-a)}}{\sqrt{(b-t)}}, & \text{near } t = b \end{cases} \tag{3.41}$$

and the integral equation (3.39) can be evaluated by using the method given in (Muskhelishvili 1953)

$$\frac{1}{\pi} \int_a^b \frac{f(t)}{(t-r)} dt = \frac{e^{i\pi/2} F^*(a)}{\sin \frac{\pi}{2} \sqrt{(b-a)(r-a)}} - \frac{F^*(b)}{\sin \frac{\pi}{2} \sqrt{(b-a)(r-b)}} + L^*(r) \tag{3.42}$$

where  $L^*(r)$  is the bounded part of the integral equation (3.42) for  $(a < r < b)$ . As  $r$  approaches  $a$ , the second part of the integral equation (3.42) will be bounded too. Therefore, the integral equation (3.42) becomes

$$\frac{1}{\pi} \int_a^b \frac{f(t)}{(t-r)} dt = \frac{F^*(a)}{\sqrt{(b-a)(r-a)}} + L^{**}(r) \quad (3.43)$$

where  $L^{**}(r)$  contains all the bounded parts of the integral equation. Now the stress intensity factors given by the equation (3.38) can be expressed in term of the unknown function  $F^*(t)$ . And by substituting the equation (3.39) and the equation (3.43) into the equation (3.38), the stress intensity factors can be found as

$$\begin{aligned} k_1(a) &= \frac{4\mu F^*(a)}{(K+1)\sqrt{\frac{b-a}{2}}}, \\ k_1(b) &= -\frac{4\mu F^*(b)}{(K+1)\sqrt{\frac{b-a}{2}}}, \end{aligned} \quad (3.44a-b)$$

To find the normalized stress intensity factors  $\bar{k}_1(a)$  and  $\bar{k}_1(b)$ , the dimensionless form of the  $F^*(t)$  will be used. Comparing the equation (3.26) and the equation (3.41), it can be related  $F^*(t)$  and  $\bar{F}^*(\tau)$  by

$$F^*(t) = \left(\frac{b-a}{2}\right) \bar{F}^*(\tau) \quad (-1 < \tau < 1) \quad (3.45)$$

By substituting the equation (3.45) into the equation (3.44), the normalized stress intensity factors  $\bar{k}_1(a)$  and  $\bar{k}_1(b)$  becomes

$$\begin{aligned} \bar{k}_1(a) &= \frac{4\mu}{\bar{p}(\xi)(K+1)} \bar{F}^*(-1), \\ \bar{k}_1(b) &= -\frac{4\mu}{\bar{p}(\xi)(K+1)} \bar{F}^*(1). \end{aligned} \quad (3.46a-b)$$

### 3.4.2 Stress Intensity Factors at the Tips of Crack Terminating at Rigid Surface

Using a similar procedure used in the previous section the normalized stress intensity factors  $\bar{k}_1(a)$  and  $\bar{k}_1(b)$  can be obtained as (Birinci 2002).



$$\begin{aligned}\bar{k}_1(a) &= \frac{4\mu}{\bar{p}(\xi)(K+1)} 2^{\frac{1}{2}-\gamma} \bar{F}^*(-1), \\ \bar{k}_1(b) &= -\frac{4\mu}{\bar{p}(\xi)(K+1)} q \bar{F}^*(1).\end{aligned}\tag{3.47a-b}$$

where

$$q = \frac{(K+1) \left[ \frac{(1-2\gamma)}{K} + 2\gamma - 3 \right]}{2 \sin \pi\gamma}\tag{3.48}$$

### 3.4.3 Stress Intensity Factor at the Tip of Internal Edge Crack

Following a similar procedure as in Section 3.4.1, it can be obtained that

$$\bar{k}_1(b) = -\frac{4\mu}{\bar{p}(\xi)(K+1)} \bar{F}^*(1).\tag{3.49}$$

## CHAPTER 4

### NUMERICAL RESULTS AND DISCUSSION

Normalized stress intensity factors  $\overline{k}_1(a)$  and  $\overline{k}_1(b)$  are calculated for various geometric configurations. Results are obtained for the following load distributions on crack surfaces:

$$\begin{aligned} p_0(r) &= p_o \\ p_1(r) &= \frac{3(b^2 - a^2)(r - B)}{2b^3 - 3Bb^2 - 2a^3 + 3Ba^2} p_o \end{aligned} \quad (4.1a-b)$$

where  $p_o$  is the mean of compressive distributed load on crack surfaces. The uniform pressure on crack surfaces is considered for the purpose of possible comparisons; since extensive numbers of examples with uniform load that appear in the literature. The outer wall is rigidly fixed while the inner surface is stress free. It is obvious that stress distribution at the location of crack for infinite cylinder loaded at infinity will not be uniform. It will vary with radial coordinate  $r$ . In order to present additional useful results one may expect for the perturbation problem in such situations where the infinite cylinder is loaded at infinity, here linearly varying load distribution on the crack surfaces are also considered.

In numerical calculations, one needs to define dimensionless load distributions as in the following form:

$$\begin{aligned} \overline{p}_0(\xi) &= p_o \\ \overline{p}_1(\xi) &= \frac{3(r_3^2 - r_2^2)((r_3 - r_2)\xi + r_3 + r_2 - 2)}{2(2r_3^3 - 3r_3^2 - 2r_2^3 + 3r_2^2)} p_o \end{aligned} \quad (4.2a-b)$$

where  $r_2 = a/B$ ,  $r_3 = b/B$ .

The following case is considered to check the formulation and the numerical results of the problem as a starting point: when the crack size becomes very small compared to other dimensions of the hollow cylinder ( $(b - a)/A = 10^{-5}$ ), the problem

turns out to be finite crack in an infinite medium and therefore the normalized stress intensity factors  $\overline{k}_1(a)$  and  $\overline{k}_1(b)$  approach unity (see Table 4.1). This is a well-known result for crack tips surrounded by a homogenous medium. Table 4.1 shows the variation of the normalized stress intensity factors  $\overline{k}_1(a)$  and  $\overline{k}_1(b)$  for an internal crack in thick-walled cylinder.

Table 4.1. Variation of the normalized stress intensity factors for an internal crack in the thick-walled cylinder ( $A/B = 0.25, \nu = 0.3$ ) for load distribution of  $p_0(r) = p_0$ .

$\frac{b-a}{A}$	$\overline{k}_1(a)$	$\overline{k}_1(b)$
$10^{-5}$	1.000000	1.000000
<b>0.2</b>	1.009990	0.990367
<b>0.4</b>	1.020380	0.980565
<b>0.6</b>	1.031450	0.970255
<b>0.8</b>	1.043670	0.959180
<b>1</b>	1.057750	0.947087
<b>1.2</b>	1.074640	0.933708
<b>1.4</b>	1.095470	0.918781
<b>1.6</b>	1.121410	0.902146
<b>1.8</b>	1.153310	0.883965

Figures 4.1-4.4 show the variation of the normalized stress intensity factors at the tips of the central crack (net ligaments,  $(a - A)$  and  $(B - b)$ , are equal) for load distributions of  $p_0(r) = p_0$  and  $p_1(r) = \frac{3(b^2 - a^2)(r - B)}{2b^3 - 3Bb^2 - 2a^3 + 3Ba^2} p_0$ , respectively. As the crack size is increased (the thickness of the net ligaments are decreased), the normalized stress intensity factor at the inner tip of the crack  $(\bar{k}_1(a))$  increases while the normalized stress intensity factor at the outer tip of the crack  $(\bar{k}_1(b))$  decreases.

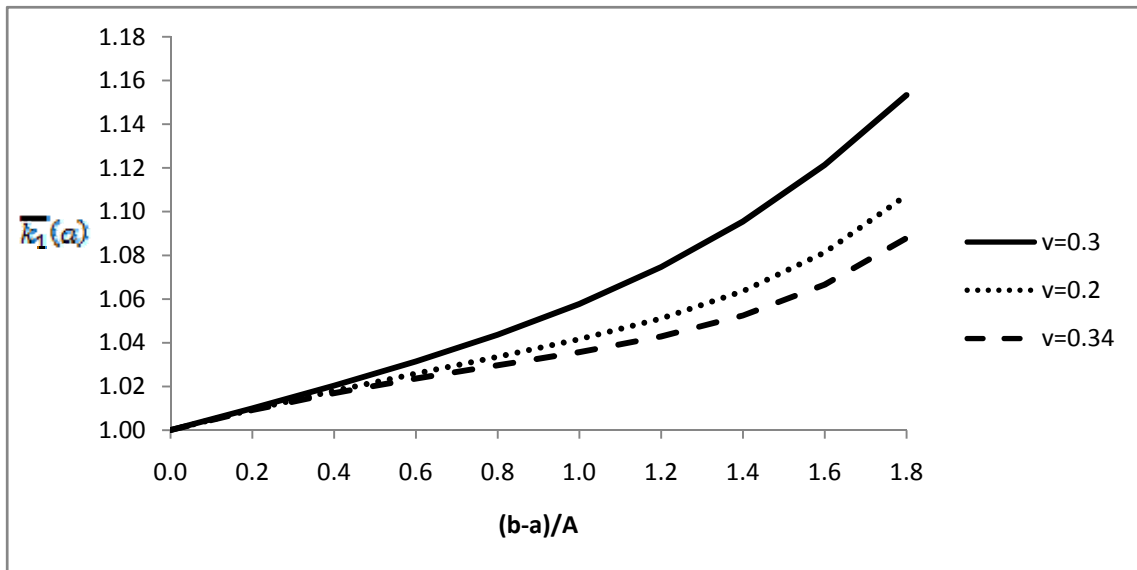


Figure 4.1. Variation of the normalized stress intensity factor  $\bar{k}_1(a)$  for an internal crack in the thick-walled cylinder ( $A/B = 0.25$ ) for uniform load distribution of  $p_0(r) = p_0$

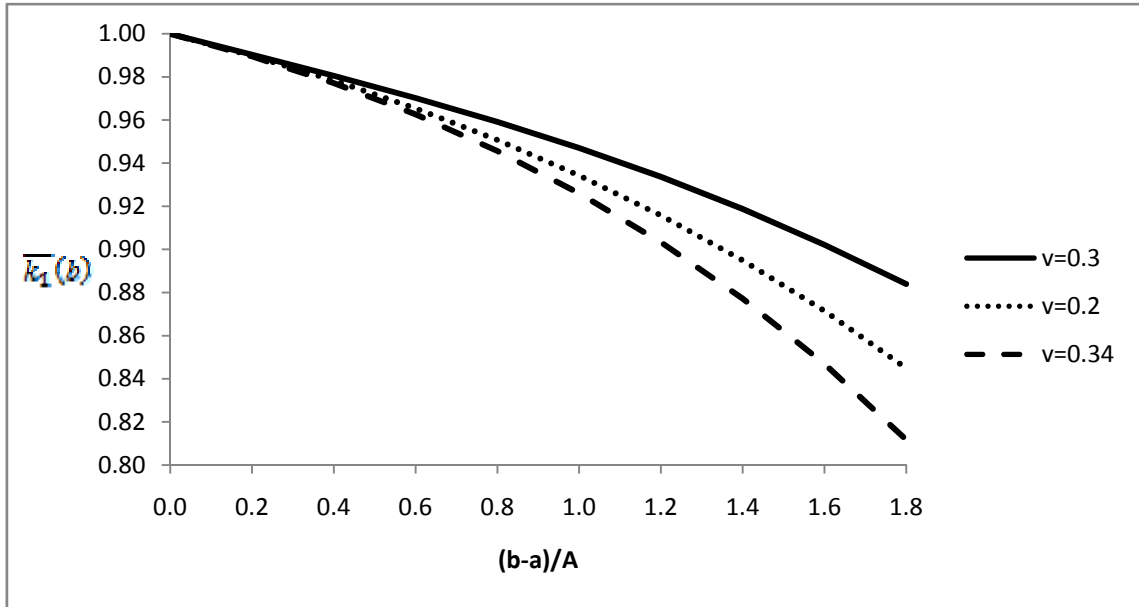


Figure 4.2. Variation of the normalized stress intensity factor  $\bar{k}_1(b)$  for an internal crack in the thick-walled cylinder ( $A/B = 0.25$ ) for uniform load distribution of  $p_0(r) = p_0$

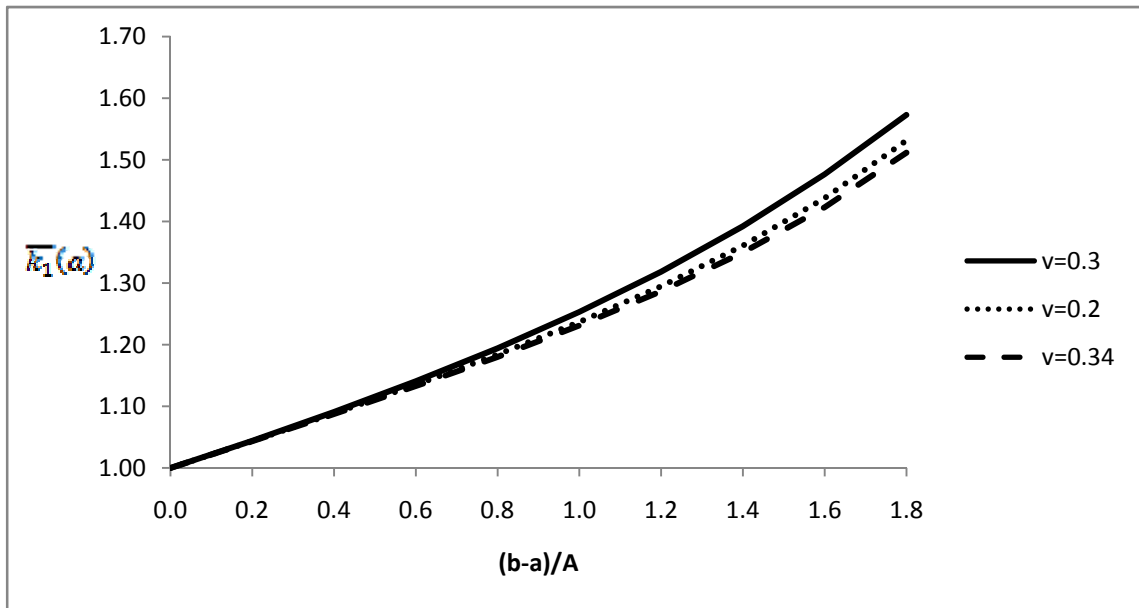


Figure 4.3. Variation of the normalized stress intensity factor  $\bar{k}_1(a)$  for an internal crack in the thick-walled cylinder ( $A/B = 0.25$ ) for linear load distribution of  $p_1(r) = \frac{3(b^2 - a^2)(r - B)}{2b^3 - 3Bb^2 - 2a^3 + 3Ba^2} p_0$

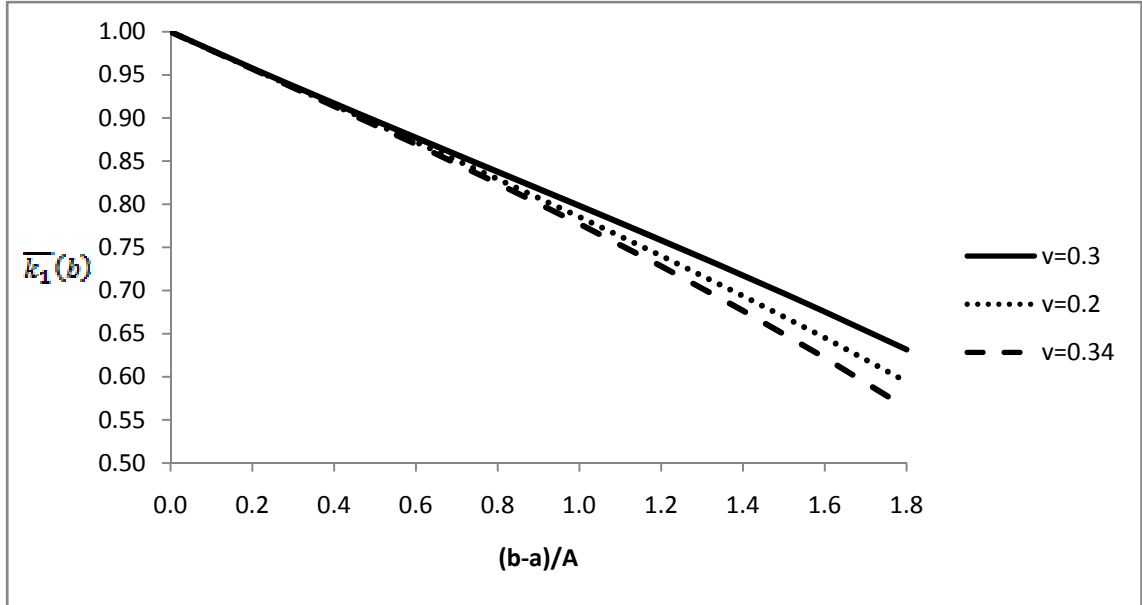


Figure 4.4. Variation of the normalized stress intensity factor  $\bar{k}_1(b)$  for an internal crack in the thick-walled cylinder ( $A/B = 0.25$ ) for linear load distribution of  $p_1(r) = \frac{3(b^2 - a^2)(r - B)}{2b^3 - 3Bb^2 - 2a^3 + 3Ba^2} p_0$

Figures 4.5-4.6 show the comparison of the stress intensity factors at the tips of the central crack (net ligaments,  $(a - A)$  and  $(B - b)$ , are equal) for load distributions of  $p_0(r) = p_0$  and  $p_1(r) = \frac{3(b^2 - a^2)(r - B)}{2b^3 - 3Bb^2 - 2a^3 + 3Ba^2} p_0$  with  $\nu=0.3$ .

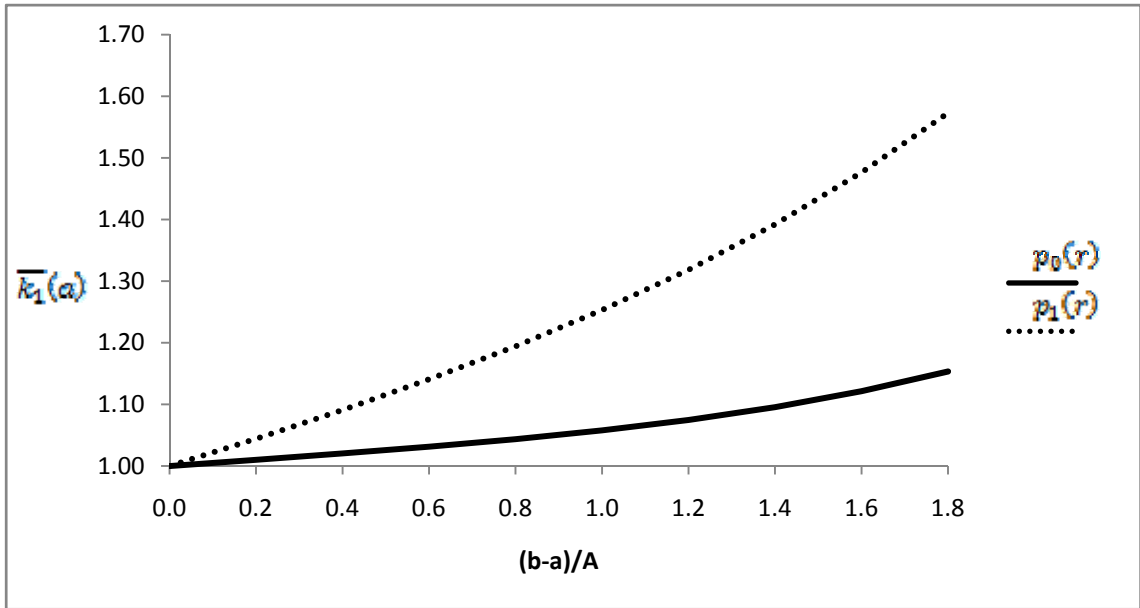


Figure 4.5. Variation of the normalized stress intensity factor  $\bar{k}_1(a)$  for an internal crack in the thick-walled cylinder ( $A/B = 0.25$ ,  $\nu = 0.3$ ) for load distributions of  $p_0(r) = p_0$  and  $p_1(r) = \frac{3(b^2 - a^2)(r - B)}{2b^3 - 3Bb^2 - 2a^3 + 3Ba^2} p_0$

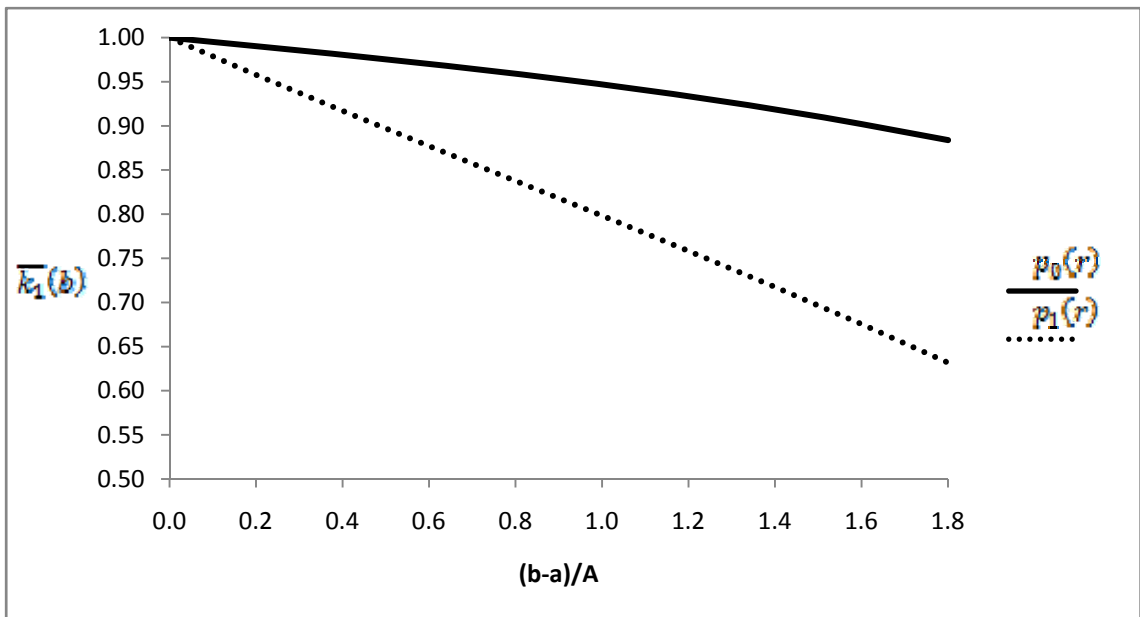


Figure 4.6. Variation of the normalized stress intensity factor  $\bar{k}_1(b)$  for an internal crack in the thick-walled cylinder ( $A/B = 0.25$ ,  $\nu = 0.3$ ) for load distributions of  $p_0(r) = p_0$  and  $p_1(r) = \frac{3(b^2 - a^2)(r - B)}{2b^3 - 3Bb^2 - 2a^3 + 3Ba^2} p_0$

Figures 4.7-4.10 show the variation of the normalized stress intensity factors at the tips of the internal crack for uniform load distribution of  $p_0(r) = p_0$  and for linear load distribution of  $p_1(r) = \frac{3(b^2 - a^2)(r - B)}{2b^3 - 3Bb^2 - 2a^3 + 3Ba^2} p_0$ . As the outer tip of the crack approaches to the outer wall of the hollow cylinder while the inner tip of the crack is being held constant ( $b/A$  increases from 2.5 to 3.4,  $a/A = 1.6$ ), the normalized stress intensity factor at the inner tip of the crack ( $\bar{k}_1(a)$ ) increases while the normalized stress intensity factor at the outer tip of the crack ( $\bar{k}_1(b)$ ) decreases.

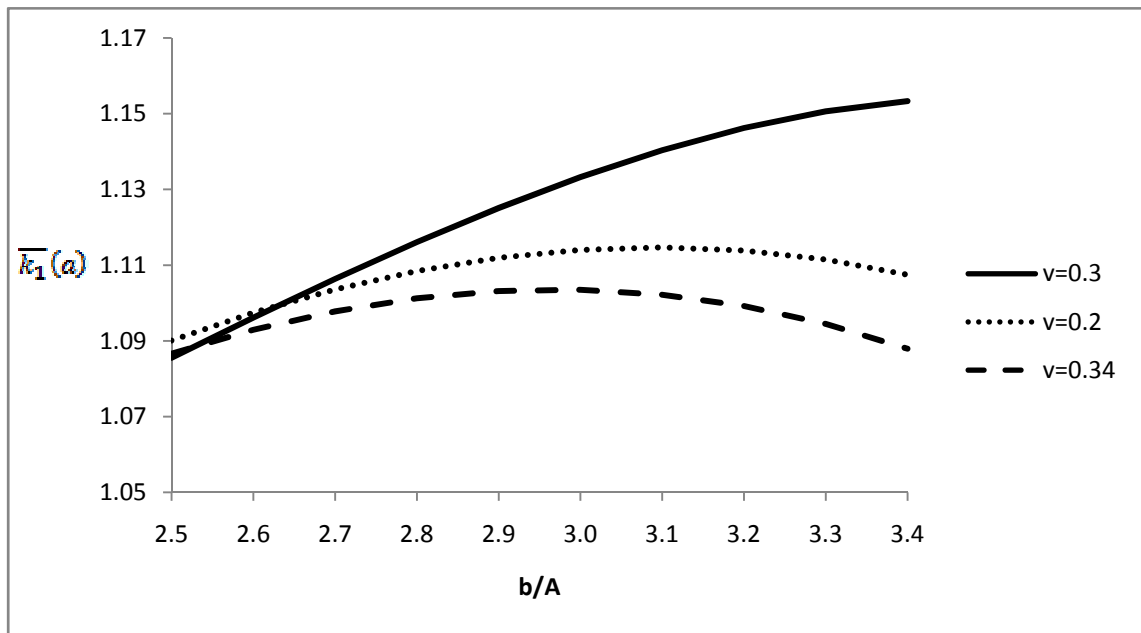


Figure 4.7. Variation of the normalized stress intensity factor  $\bar{k}_1(a)$  for an internal crack in the thick-walled cylinder ( $A/B = 0.25$ ,  $a/A = 1.6$ ) for uniform load distribution of  $p_0(r) = p_0$



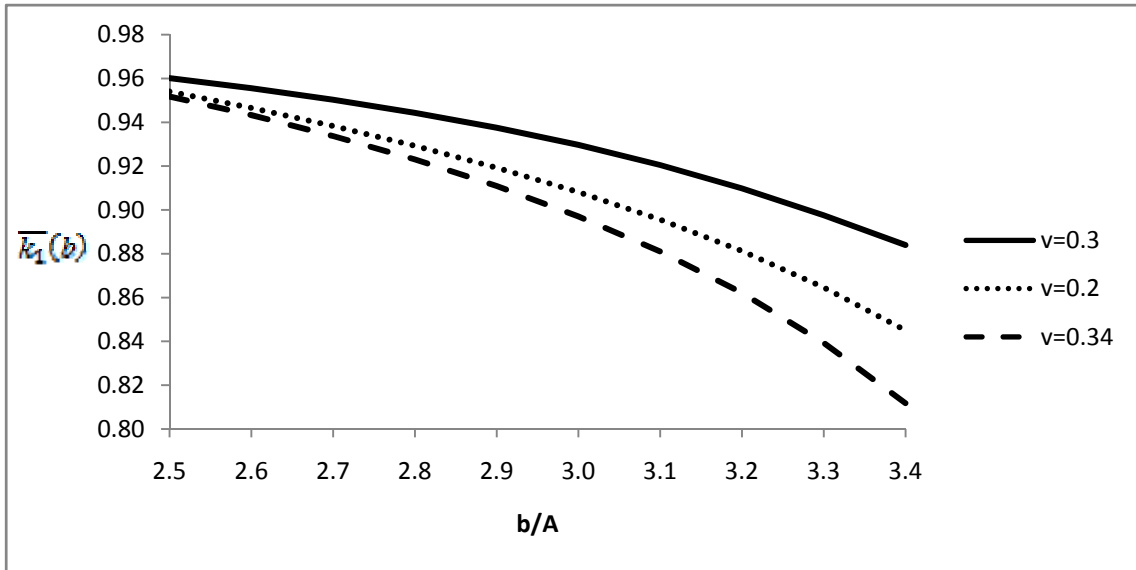


Figure 4.8. Variation of the normalized stress intensity factor  $\bar{k}_1(b)$  for an internal crack in the thick-walled cylinder ( $A/B = 0.25$ ,  $a/A = 1.6$ ) for uniform load distribution of  $p_0(r) = p_0$

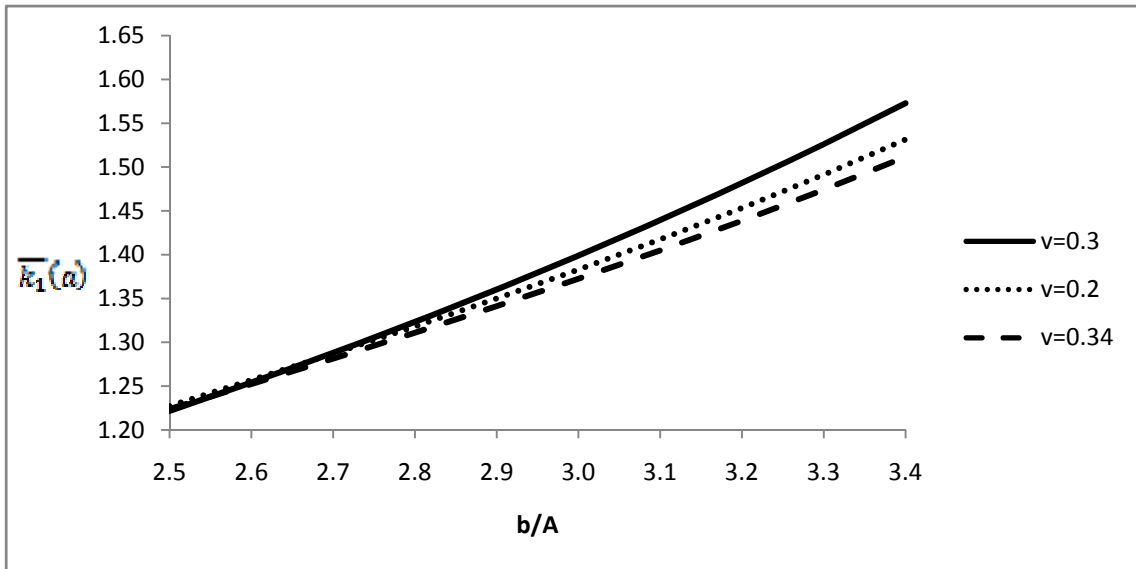


Figure 4.9. Variation of the normalized stress intensity factor  $\bar{k}_1(a)$  for an internal crack in the thick-walled cylinder ( $A/B = 0.25$ ,  $a/A = 1.6$ ) for load distribution of  $p_1(r) = \frac{3(b^2 - a^2)(r - B)}{2b^3 - 3Bb^2 - 2a^3 + 3Ba^2} p_0$

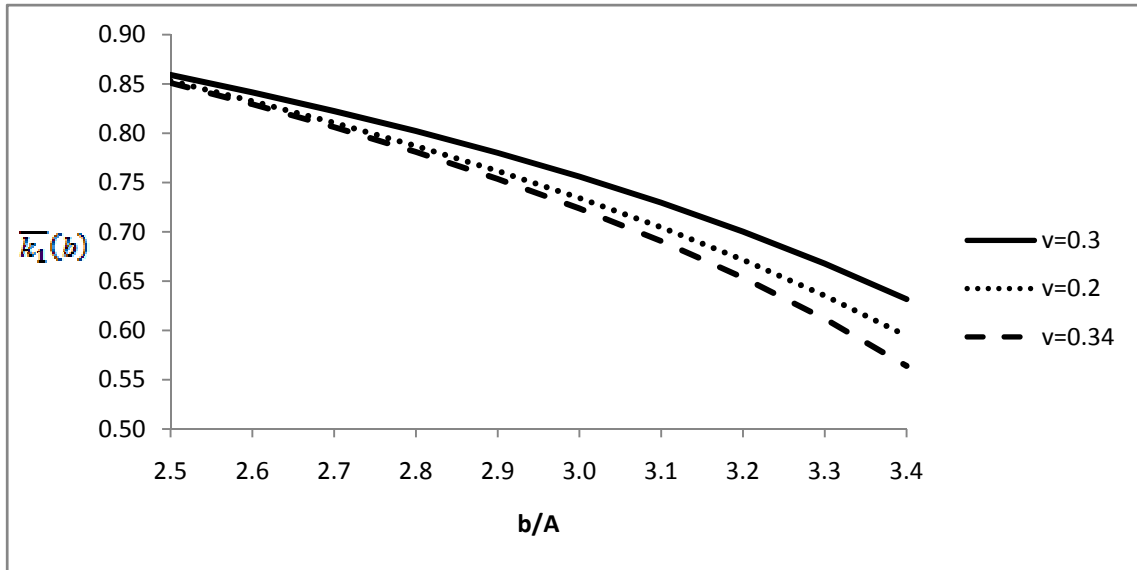


Figure 4.10. Variation of the normalized stress intensity factor  $\bar{k}_1(b)$  for an internal crack in the thick-walled cylinder ( $A/B = 0.25, a/A = 1.6$ ) for load distribution of  $p_1(r) = \frac{3(b^2 - a^2)(r - B)}{2b^3 - 3Bb^2 - 2a^3 + 3Ba^2} p_0$

Figures 4.11-4.12 show the comparison of the stress intensity factors at the tips of the internal crack for uniform load distribution of  $p_0(r) = p_0$  and linear load distribution of  $p_1(r) = \frac{3(b^2 - a^2)(r - B)}{2b^3 - 3Bb^2 - 2a^3 + 3Ba^2} p_0$  as the outer tip of the crack approaches to the outer wall of the hollow cylinder while the inner tip of the crack is being held constant.

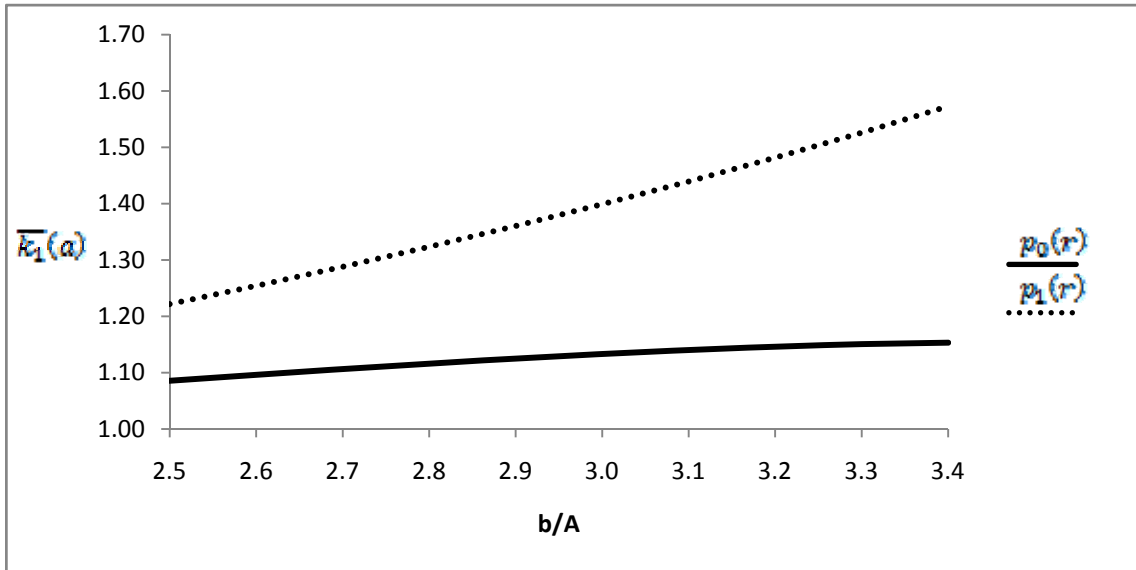


Figure 4.11. Variation of the normalized stress intensity factor  $\bar{k}_1(a)$  for an internal crack in the thick-walled cylinder ( $A/B = 0.25$ ,  $\nu = 0.3$ ,  $a/A = 1.6$ ) for load distributions of  $p_0(r) = p_0$  and  $p_1(r) = \frac{3(b^2 - a^2)(r - B)}{2b^3 - 3Bb^2 - 2a^3 + 3Ba^2} p_0$

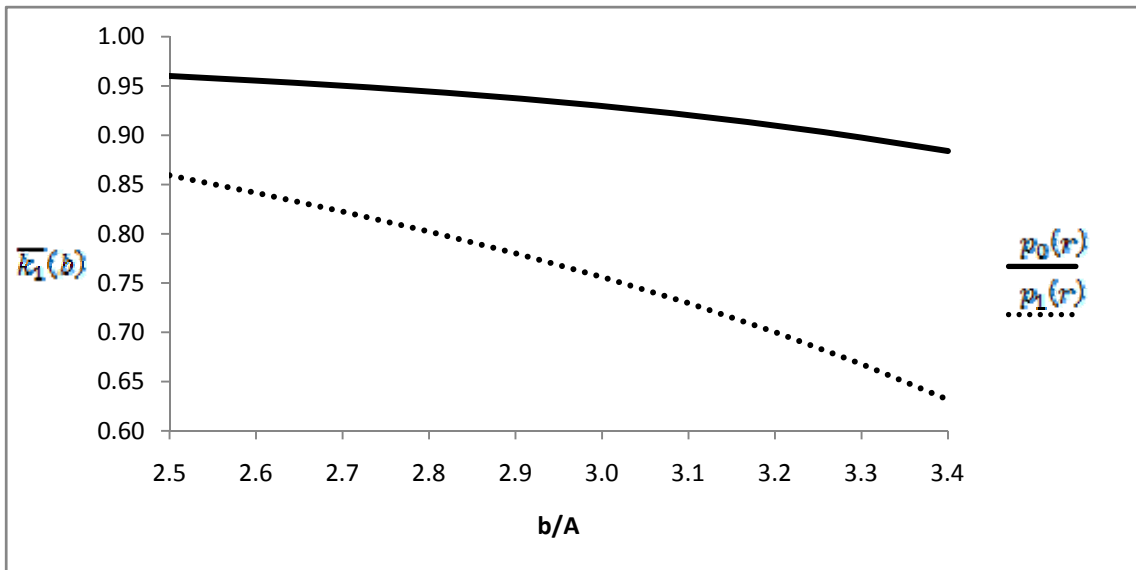


Figure 4.12. Variation of the normalized stress intensity factor  $\bar{k}_1(b)$  for an internal crack in the thick-walled cylinder ( $A/B = 0.25$ ,  $\nu = 0.3$ ,  $a/A = 1.6$ ) for load distributions of  $p_0(r) = p_0$  and  $p_1(r) = \frac{3(b^2 - a^2)(r - B)}{2b^3 - 3Bb^2 - 2a^3 + 3Ba^2} p_0$

Figures 4.13-4.16 show the variation of the normalized stress intensity factors at the tips of the internal crack for uniform load distribution of  $p_0(r) = p_o$  and linear load distribution of  $p_1(r) = \frac{3(b^2-a^2)(r-B)}{2b^3-3Bb^2-2a^3+3Ba^2} p_o$ . As the inner tip of the crack approaches to the inner wall of the hollow cylinder while the outer tip of the crack is being held constant ( $a/A$  increases from 1.6 to 2.5,  $b/A = 3.4$ ), the normalized stress intensity factor at the inner tip of the crack ( $\bar{k}_1(a)$ ) decreases while the normalized stress intensity factor at the outer tip of the crack ( $\bar{k}_1(b)$ ) increases.

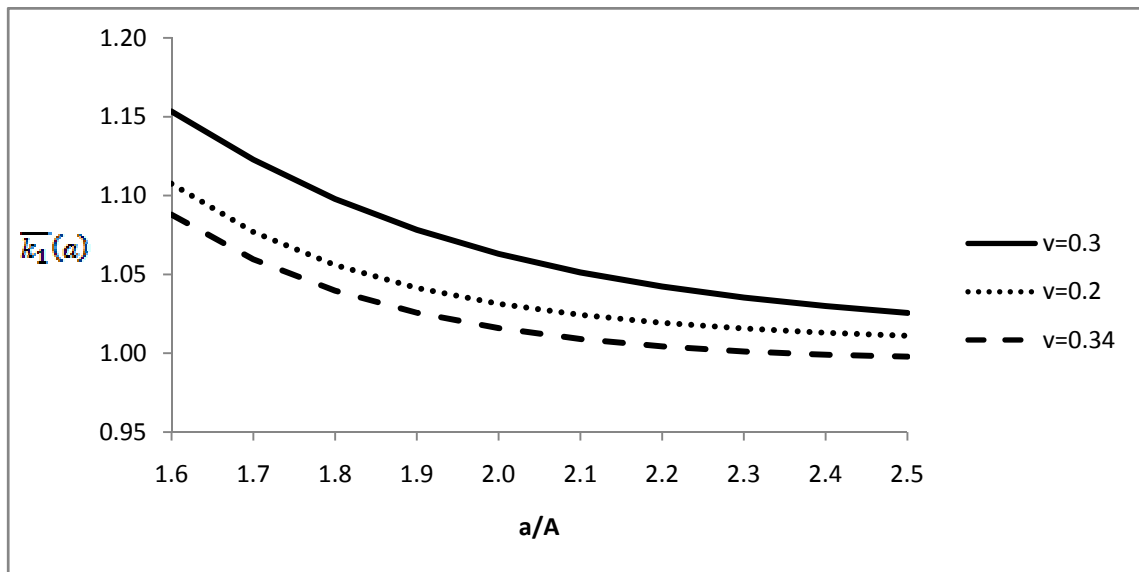


Figure 4.13. Variation of the normalized stress intensity factor  $\bar{k}_1(a)$  for an internal crack in the thick-walled cylinder ( $A/B = 0.25$ ,  $b/A = 3.4$ ) for uniform load distribution of  $p_0(r) = p_o$

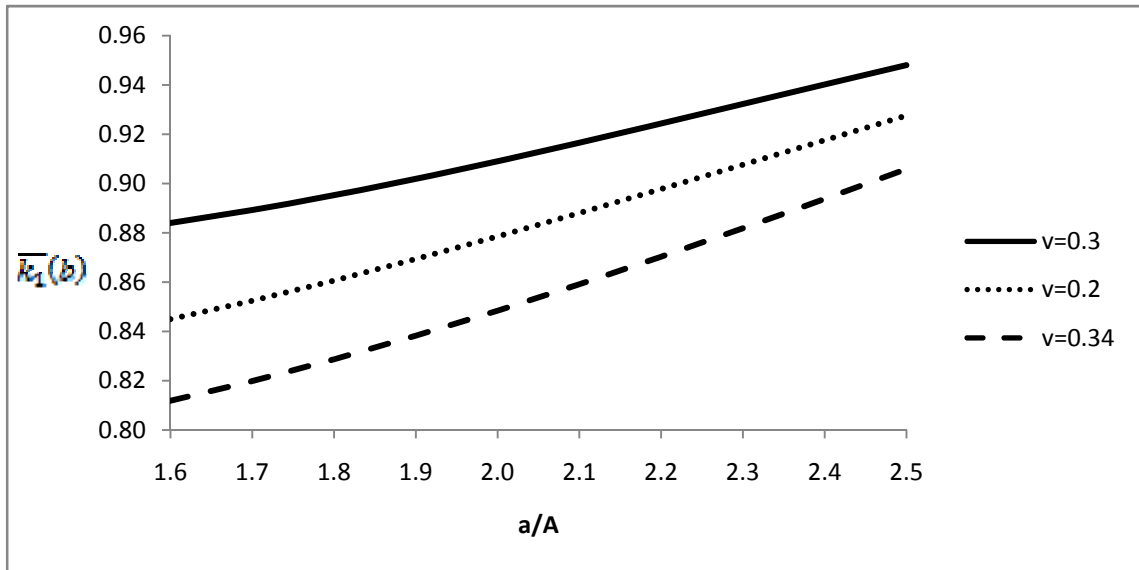


Figure 4.14. Variation of the normalized stress intensity factor  $\bar{k}_1(b)$  for an internal crack in the thick-walled cylinder ( $A/B = 0.25$ ,  $b/A = 3.4$ ) for uniform load distribution of  $p_0(r) = p_0$

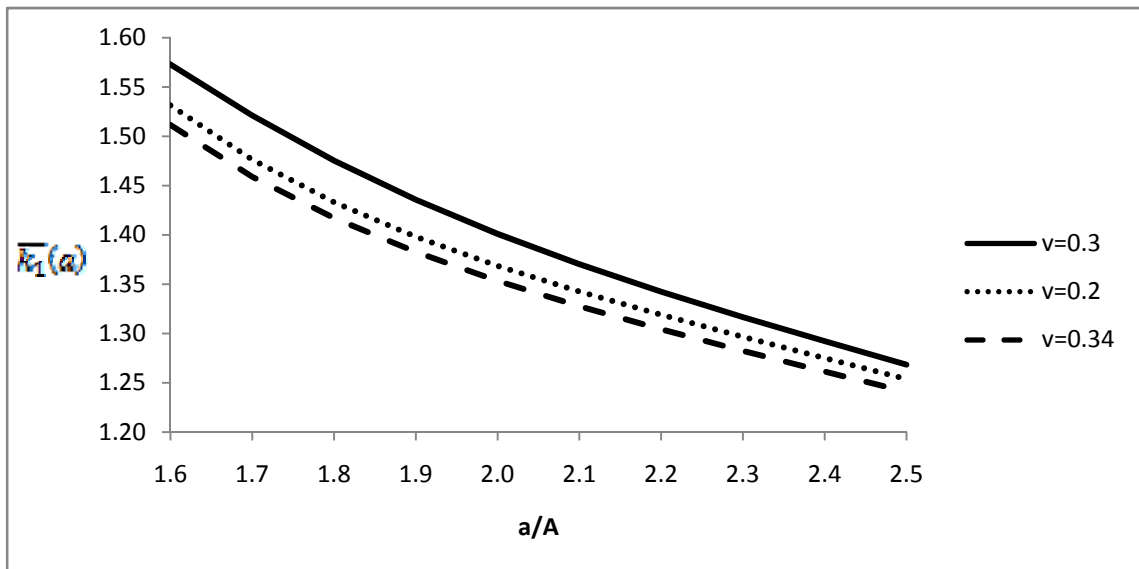


Figure 4.15. Variation of the normalized stress intensity factor  $\bar{k}_1(a)$  for an internal crack in the thick-walled cylinder ( $A/B = 0.25$ ,  $b/A = 3.4$ ) for load distribution of  $p_1(r) = \frac{3(b^2 - a^2)(r - B)}{2b^3 - 3Bb^2 - 2a^3 + 3Ba^2} p_0$

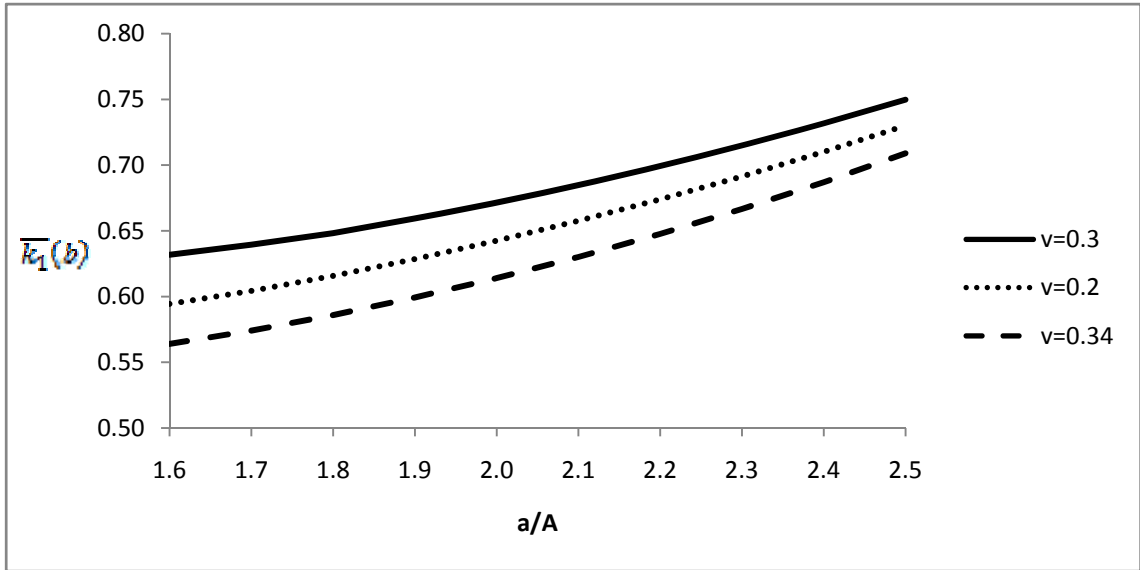


Figure 4.16. Variation of the normalized stress intensity factor  $\bar{k}_1(b)$  for an internal crack in the thick-walled cylinder ( $A/B = 0.25, b/A = 3.4$ ) for load distribution of  $p_1(r) = \frac{3(b^2 - a^2)(r - B)}{2b^3 - 3Bb^2 - 2a^3 + 3Ba^2} p_0$

Figures 4.17-4.18 show comparison of stress intensity factors at the tips of the internal crack for load distributions of  $p_0(r) = p_0$  and  $p_1(r) = \frac{3(b^2 - a^2)(r - B)}{2b^3 - 3Bb^2 - 2a^3 + 3Ba^2} p_0$  as the inner tip of the crack approaches to the inner wall of the hollow cylinder while the outer tip of the crack is being held constant.

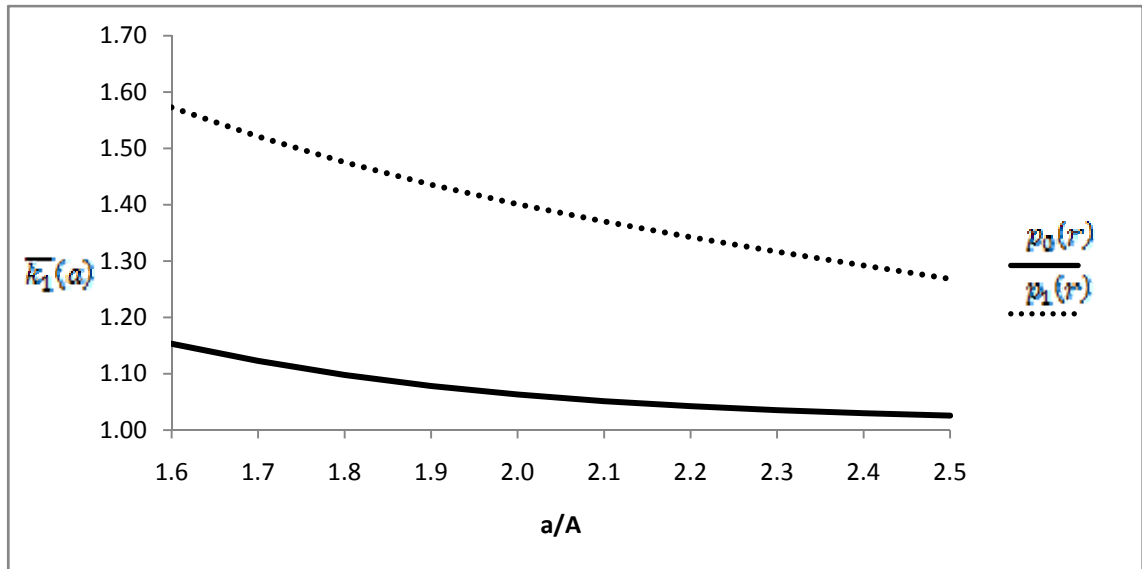


Figure 4.17. Variation of the normalized stress intensity factor  $\bar{k}_1(a)$  for an internal crack in the thick-walled cylinder ( $A/B = 0.25$ ,  $\nu = 0.3$ ,  $b/A = 3.4$ ) for load distributions of  $p_0(r) = p_0$  and  $p_1(r) = \frac{3(b^2 - a^2)(r - B)}{2b^3 - 3Bb^2 - 2a^3 + 3Ba^2} p_0$

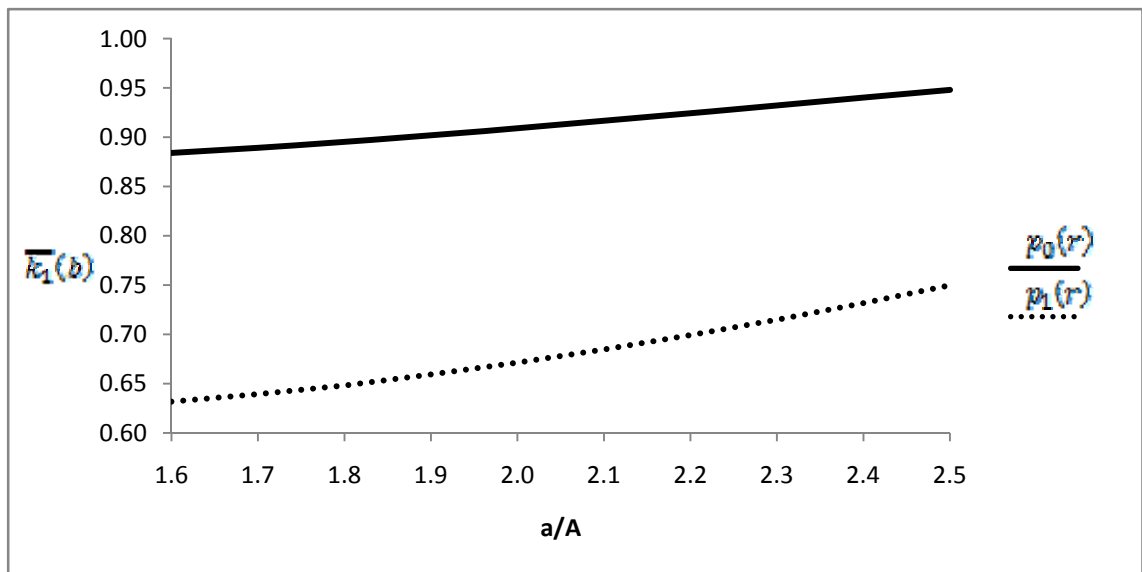


Figure 4.18. Variation of the normalized stress intensity factor  $\bar{k}_1(b)$  for an internal crack in the thick-walled cylinder ( $A/B = 0.25$ ,  $\nu = 0.3$ ,  $b/A = 3.4$ ) for load distributions of  $p_0(r) = p_0$  and  $p_1(r) = \frac{3(b^2 - a^2)(r - B)}{2b^3 - 3Bb^2 - 2a^3 + 3Ba^2} p_0$

Figures 4.19-4.22 show the variation of normalized stress intensity factors  $\bar{k}_1(a)$  and  $\bar{k}_1(b)$  at the tips of the crack terminating at the rigid surface. As  $a/A$  increases (crack gets further from the free inner surface),  $\bar{k}_1(a)$  decreases considerably more than  $\bar{k}_1(b)$  for all values of  $\nu=0.2, \nu=0.3, \nu=0.34$ .

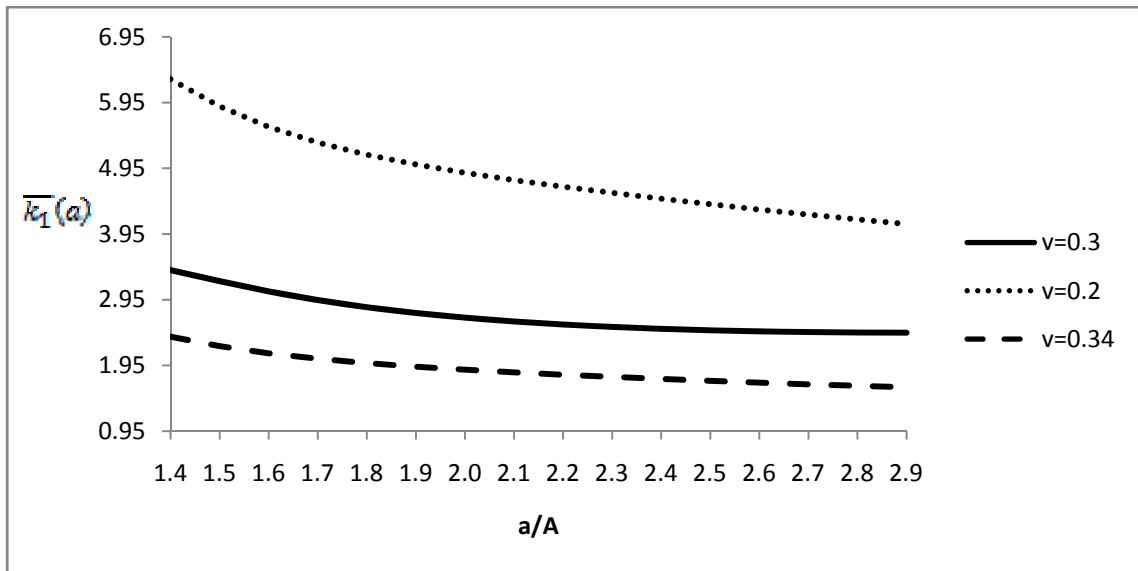


Figure 4.19. Variation of the normalized stress intensity factor  $\bar{k}_1(a)$  for a crack terminating at rigid surface in the thick-walled cylinder ( $A/B = 0.25, b/B = 1$ ) for load distribution of  $p_0(r) = p_o$



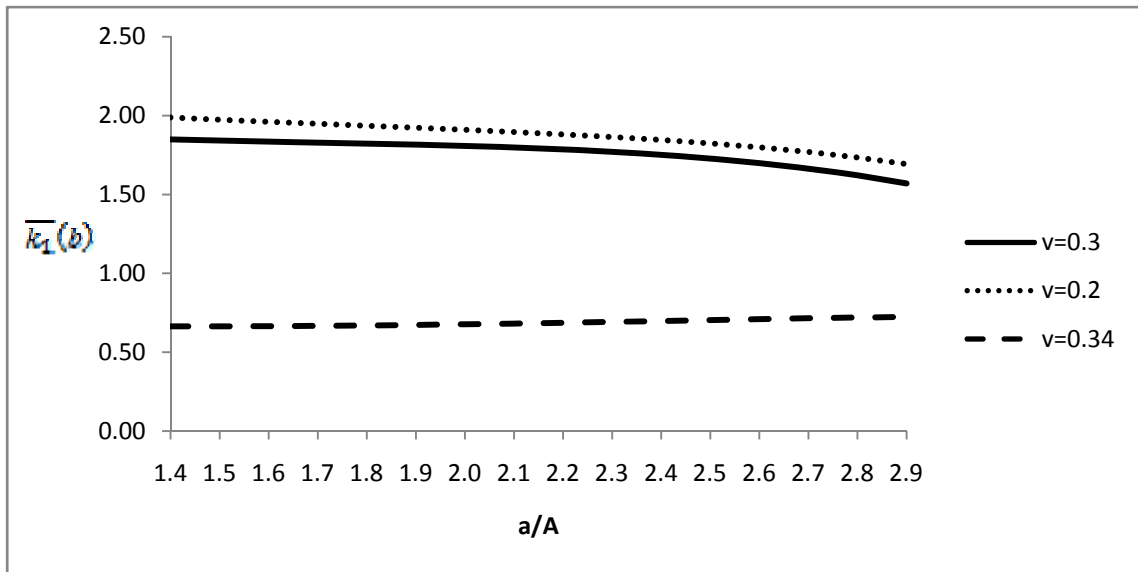


Figure 4.20. Variation of the normalized stress intensity factor  $\bar{k}_1(b)$  for a crack terminating at rigid surface in the thick-walled cylinder ( $A/B = 0.25, b/B = 1$ ) for load distribution of  $p_0(r) = p_0$

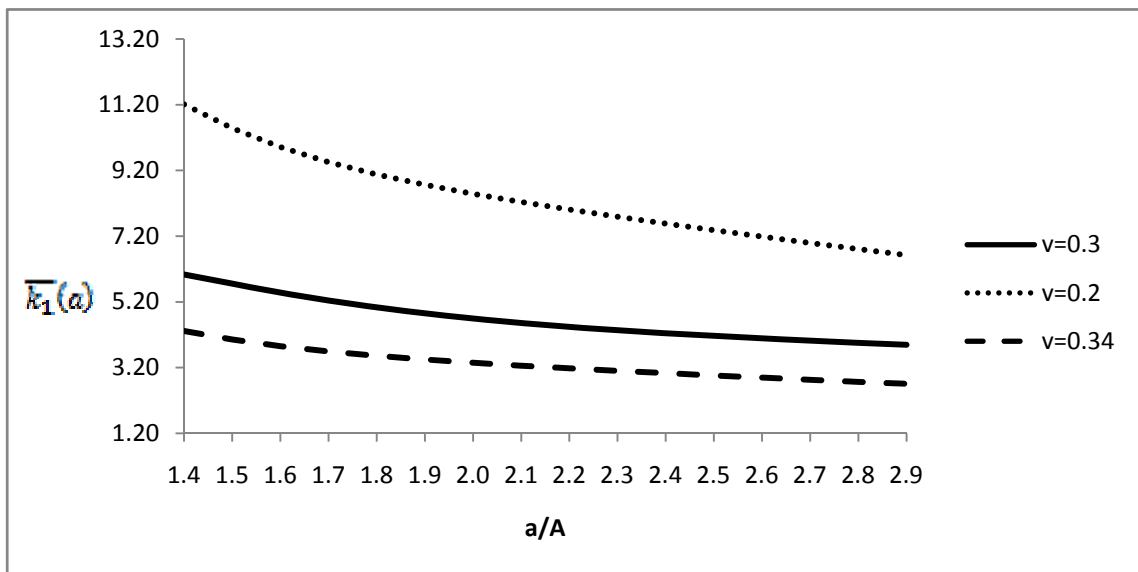


Figure 4.21. Variation of the normalized stress intensity factor  $\bar{k}_1(a)$  for a crack terminating at rigid surface in the thick-walled cylinder ( $A/B = 0.25, b/B = 1$ ) for linear load distribution of  $p_1(r) = \frac{3(b^2 - a^2)(r - B)}{2b^3 - 3Bb^2 - 2a^3 + 3Ba^2} p_0$

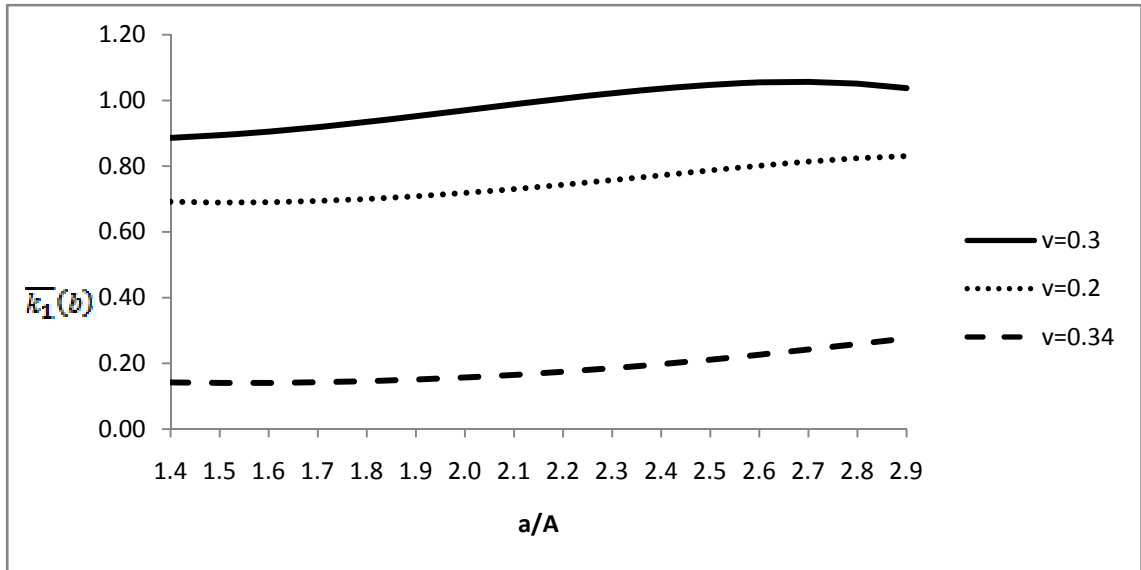


Figure 4.22. Variation of the normalized stress intensity factor  $\bar{k}_1(b)$  for a crack terminating at rigid surface in the thick-walled cylinder ( $A/B = 0.25, b/B = 1$ ) for linear load distribution of  $p_1(r) = \frac{3(b^2 - a^2)(r - B)}{2b^3 - 3Bb^2 - 2a^3 + 3Ba^2} p_0$

Figure 4.23 and Figure 4.24 are presented for comparison purposes for  $\nu=0.3$ .

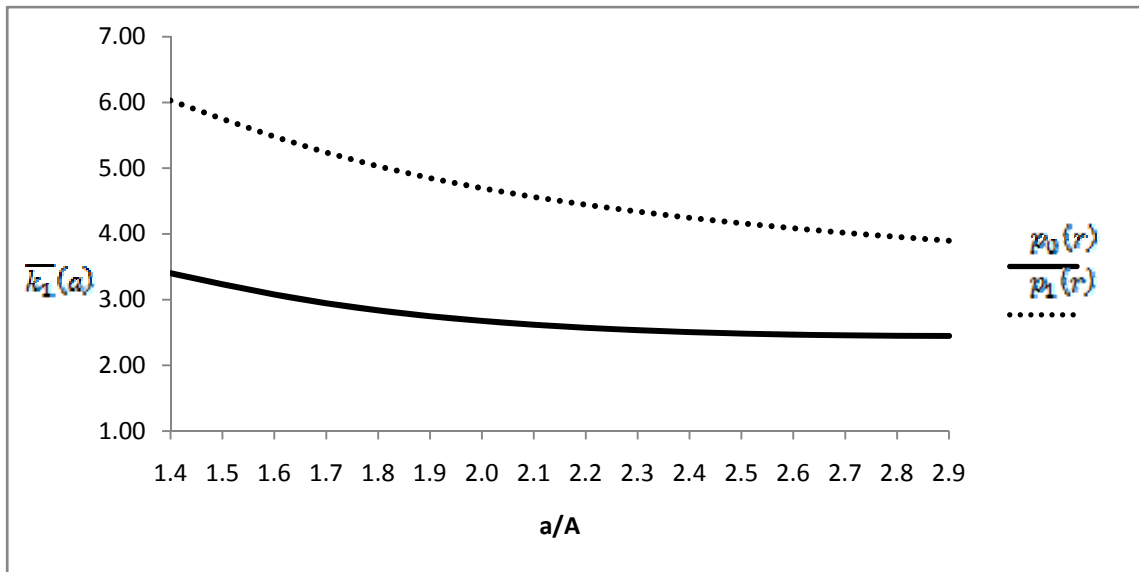


Figure 4.23. Variation of the normalized stress intensity factor  $\bar{k}_1(a)$  for a crack terminating at rigid surface ( $A/B = 0.25, \nu = 0.3, b/B = 1$ ) for load distributions of  $p_0(r) = p_0$  and  $p_1(r) = \frac{3(b^2 - a^2)(r - B)}{2b^3 - 3Bb^2 - 2a^3 + 3Ba^2} p_0$

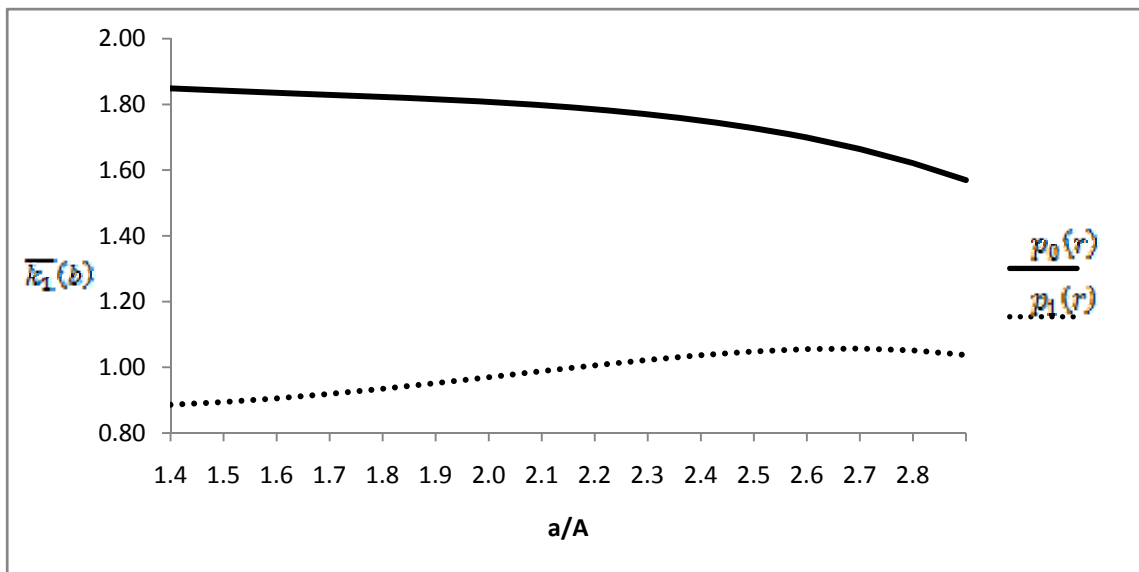


Figure 4.24. Variation of the normalized stress intensity factor  $\bar{k}_1(b)$  for a crack terminating at rigid surface ( $A/B = 0.25, \nu = 0.3, b/B = 1$ ) for load distributions of  $p_0(r) = p_0$  and  $p_1(r) = \frac{3(b^2 - a^2)(r - B)}{2b^3 - 3Bb^2 - 2a^3 + 3Ba^2} p_0$

When  $a/A = 1$  and  $b/A$  increases (crack tip gets closer to the rigid surface),  $\bar{k}_1(b)$  increases initially while the crack length has relatively small values, then decreases slightly. This can be seen in Figure 4.25 and Figure 4.26.

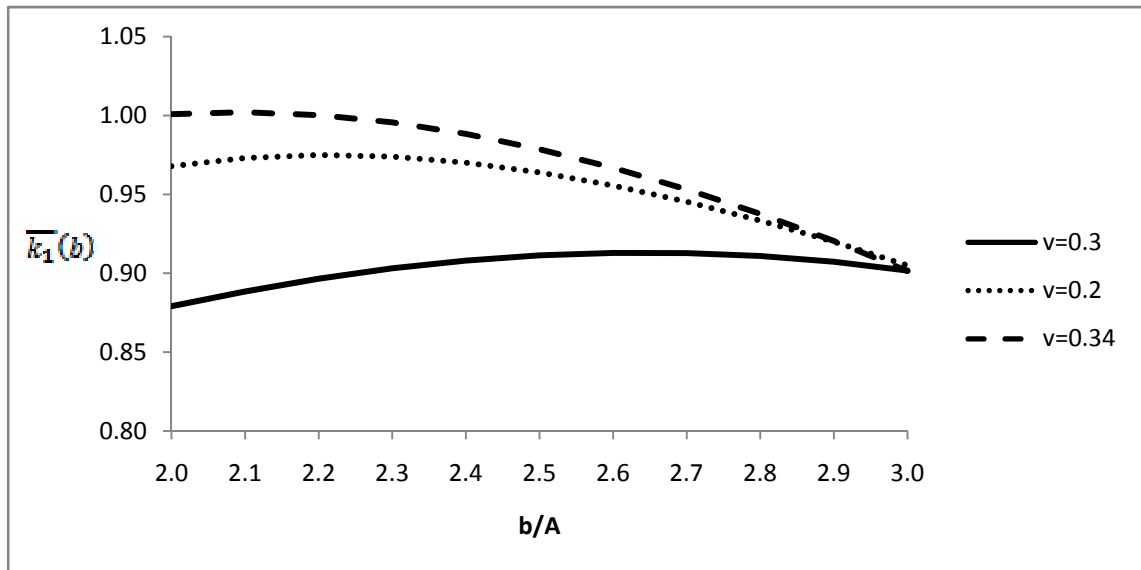


Figure 4.25. Variation of the normalized stress intensity factor  $\bar{k}_1(b)$  for an internal edge crack in the thick-walled cylinder ( $A/B = 0.25$ ,  $a/A = 1$ ) for load distribution of  $p_0(r) = p_0$

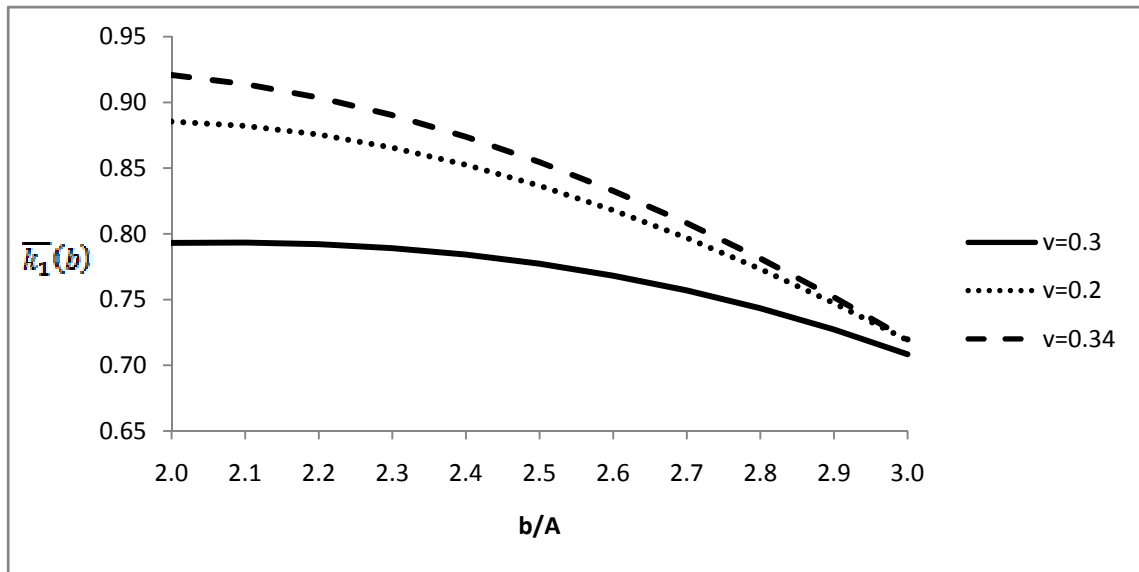


Figure 4.26. Variation of the normalized stress intensity factor  $\bar{k}_1(b)$  for an internal edge crack in the thick-walled cylinder ( $A/B = 0.25, a/A = 1$ ) for load distribution of  $p_1(r) = \frac{3(b^2 - a^2)(r - B)}{2b^3 - 3Bb^2 - 2a^3 + 3Ba^2} p_0$

Variation of  $\bar{k}_1(b)$  for uniform and linear loadings with  $\nu=0.3$  for an internal edge crack is shown in Figure 4.27 for comparison purposes.

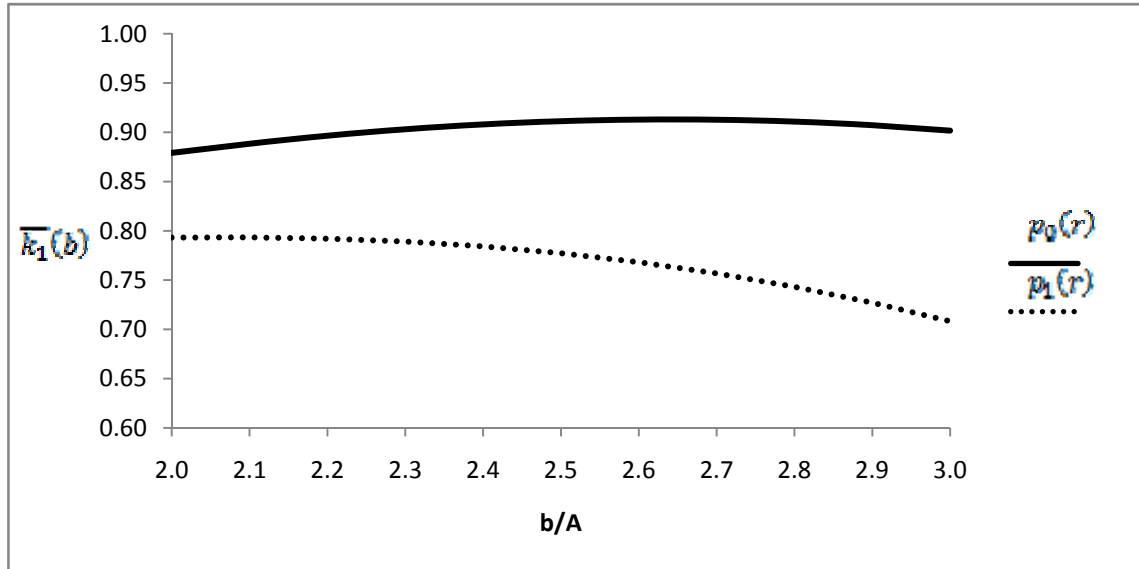


Figure 4.27. Variation of the normalized stress intensity factor  $\bar{k}_1(b)$  for an internal edge crack in the thick-walled cylinder ( $A/B = 0.25$ ,  $\nu = 0.3$ ,  $a/A = 1$ ) for load distributions of  $p_0(r) = p_0$  and  $p_1(r) = \frac{3(b^2 - a^2)(r - B)}{2b^3 - 3Bb^2 - 2a^3 + 3Ba^2} p_0$

## CHAPTER 5

### CONCLUSION

In this thesis, the stress intensity factors for an infinite hollow cylinder at the tips of the crack is calculated for an internal crack (embedded), a crack terminating at the rigid surface and internal edge crack. Problem is defined and modelled in terms of a linear second order partial differential equation system with mixed boundary conditions. Integral transform techniques are used to solve these governing equations that are reduced to a singular integral equation. Solving this singular integral equation numerically, normalized stress intensity factors are calculated for various geometric conditions and for various Poisson's ratio. Numerical results are presented in graphical forms.

The following results are concluded:

1. It is observed that  $\overline{k_1}(a)$  is always greater than  $\overline{k_1}(b)$ .
2. As the outer crack tip approaches the rigid wall ( $b$  increases),  $\overline{k_1}(b)$  decreases because rigid wall prevents the crack opening.
3. As the inner crack tip approaches the stress free surface ( $a$  increases),  $\overline{k_1}(a)$  increases since the free lateral surface lets the crack open.
4. The results are also compared for uniform and linear loadings applied on crack surfaces. Both showed the similar behaviour for stress intensity factors at the crack tips.
5. It is observed that, stress intensity factors are affected by Poisson's ratio as a material property.

## REFERENCES

- Abramowitz, M., and I.A. Stegun. 1965. *Handbook of Mathematical Functions*. Dover.
- Agarwal, Y.K. 1978. Axisymmetric Solution of the End Problem for a Semi-Infinite Elastic Circular Cylinder and Its Application to Joined Dissimilar Cylinders under Uniform Tension. *International Journal of Engineering Science*: 985-998.
- Arin, K., and F. Erdoğan. 1971. Penny-Shaped Crack in an Elastic Layer Bonded to Dissimilar Half Spaces. *International Journal of Engineering Science*: 213-232.
- Artem, H.S.A., and M.R. Geçit. 2002. An Elastic Hollow Cylinder under Axial Tension Containing a Crack and Two Rigid Inclusions of Ring Shape. *Computers and Structures*: 2277-2287.
- Aydin, L. 2005. Investigation of Stress Intensity Factors in an Elastic Cylinder under Axial Tension with a Crack of Ring-Shape..
- Benthem, J.P., and P. Minderhoud. 1972. The Problem of the Solid Cylinder Compressed Between Rough Rigid Stamps. *International Journal of Solids and Structures*: 1027-1042.
- Birinci, A. 2002. Axisymmetric Crack Problem of a Thick-Walled Cylinder with Cladding. *International Journal of Engineering Science*: 1729-1750.
- Broek, D. 1999. *Elementary Engineering Fracture Mechanics*. Springer.
- Chen, Y.Z. 2000. Stress Intensity Factors in a Finite Length Cylinder with a Circumferential Crack. *International Journal of Pressure Vessels and Piping*: 439-444.
- Collins, W.D. 1962. Some Axially Symmetric Stress Distributions in Elastic Solids Containing Penny-Shaped Cracks. I. Cracks in an Infinite Solid and Thick Plate. *Proceedings of the Royal Society of London. Series A, Mathematical and Physical Sciences*: 359-386.
- Cook, T.S., and F Erdoğan. Stresses in Bonded Materials with a Crack Perpendicular to the Interface. *International Journal of Engineering Science*, 1972: 677-697.
- Delale, F., and F. Erdoğan. 1982. Stress Intensity Factor in a Hollow Cylinder Containing a Radial Crack. *International Journal of Fracture*: 251-265.
- Erdoğan, F. 2000. Fracture Mechanics. *International Journal of Solids and Structures*: 171-183.



- Erdoğan, F., Gupta, and T.S. Cook. 1973. *Numerical Solution of Singular Integral Equation*. Mechanics of Fracture I, Methods of Analysis and Solutions of Crack Problems, Edited by Sih, G.C., Noordhoff International Publishing Leyden: 368-425.
- Erdol, R., and F. Erdoğan. 1978. A thick-walled Cylinder with an axisymmetric Internal or Edge Crack. *Journal of Applied Mechanics*: 281-286.
- Gupta, G.D. 1974. The Analysis of Semi-Infinite Cylinder Problem. *International Journal of Solids and Structures*: 137-148.
- Isida, M., K. Hirota, H. Noguchi, and T. Yoshida. 1985. Two Parallel Elliptical Cracks in an Infinite Solid Subjected to Tension. *International Journal of Fracture*: 31-48.
- Kaman, M.O., and M.R. Gecit. 2006. Cracked semi-infinite cylinder and finite cylinder problems. *International Journal of Engineering Science*: 1534-1555.
- McLachlan, N.W. 1955. *Bessel Functions for Engineers*. Oxford University Press.
- Muskhelishvili, N.I. 1953. *Singular Integral Equations*. Groningen: P. Noordhoff.
- Nied, H.F., and Erdoğan F. 1983. The Elasticity Problem for a Thick-Walled Cylinder Containing a Circumferential Crack. *International Journal of Fracture*: 277-301.
- Sanford, R.J. 2002. *Principle of Fracture Mechanics*. Prentice Hall.
- Sih, G.C. 1973. *Handbook of SIFs: Stress Intensity Factor Solutions and Formulas for Reference*. Lehigh University Institute of Fracture and Solid Mechanics.
- Sneddon, I.N., and J.T. Welch. 1963. A note on the Distribution of Stress in a Cylinder Containing a Penny-Shaped Crack. *International Journal of Engineering Science*: 411-419.
- Timoshenko, S.P., and J.N. Goodier. 1970. *Theory of Elasticity*. McGraw-Hill International Editions.

## APPENDIX A

### INTEGRATION FORMULAS

$$\int_0^\infty \frac{\alpha}{(\alpha^2 + \lambda^2)} J_0(A\alpha) J_0(t\alpha) d\alpha = I_0(A\lambda) K_0(t\lambda) \quad (A \leq t)$$

$$\int_0^\infty \frac{\alpha^2}{(\alpha^2 + \lambda^2)} J_1(A\alpha) J_0(t\alpha) d\alpha = -\lambda I_0(A\lambda) K_0(t\lambda) \quad (A \leq t)$$

$$\int_0^\infty \frac{\alpha}{(\alpha^2 + \lambda^2)} J_1(A\alpha) J_1(t\alpha) d\alpha = I_1(A\lambda) K_1(t\lambda) \quad (A \leq t)$$

$$\int_0^\infty \frac{\alpha^2}{(\alpha^2 + \lambda^2)} J_0(A\alpha) J_1(t\alpha) d\alpha = \lambda I_0(A\lambda) K_1(t\lambda) \quad (A \leq t)$$

$$\int_0^\infty \frac{\alpha}{(\alpha^2 + \lambda^2)^2} J_0(A\alpha) J_0(t\alpha) d\alpha = \frac{1}{2\lambda} [-AI_1(A\lambda)K_0(t\lambda) + tI_0(A\lambda)K_1(t\lambda)] \quad (A \leq t)$$

$$\begin{aligned} \int_0^\infty \frac{\alpha^2}{(\alpha^2 + \lambda^2)^2} J_1(A\alpha) J_0(t\alpha) d\alpha \\ = \frac{1}{2\lambda} [\lambda AI_0(A\lambda)K_0(t\lambda) - \lambda t I_1(A\lambda)K_1(t\lambda)] \end{aligned} \quad (A \leq t)$$

$$\begin{aligned} \int_0^\infty \frac{\alpha}{(\alpha^2 + \lambda^2)^2} J_1(A\alpha) J_1(t\alpha) d\alpha \\ = \frac{1}{2\lambda} \left[ -AI_0(A\lambda)K_1(t\lambda) + \frac{2}{\lambda} I_1(A\lambda)K_1(t\lambda) + tI_1(A\lambda)K_0(t\lambda) \right] \end{aligned} \quad (A \leq t)$$

$$\begin{aligned} \int_0^\infty \frac{\alpha^2}{(\alpha^2 + \lambda^2)^2} J_0(A\alpha) J_1(t\alpha) d\alpha \\ = \frac{1}{2\lambda} [-\lambda AI_1(A\lambda)K_1(t\lambda) + \lambda t I_0(A\lambda)K_0(t\lambda)] \end{aligned} \quad (A \leq t)$$

$$\int_0^\infty \frac{\alpha}{(\alpha^2 + \lambda^2)} J_0(B\alpha) J_0(t\alpha) d\alpha = K_0(B\lambda) I_0(t\lambda) \quad (B \geq t)$$

$$\int_0^\infty \frac{\alpha^2}{(\alpha^2 + \lambda^2)} J_1(B\alpha) J_0(t\alpha) d\alpha = \lambda K_1(B\lambda) I_0(t\lambda) \quad (B \geq t)$$

$$\int_0^\infty \frac{\alpha}{(\alpha^2 + \lambda^2)} J_1(B\alpha) J_1(t\alpha) d\alpha = K_1(B\lambda) I_1(t\lambda) \quad (B \geq t)$$

$$\int_0^\infty \frac{\alpha^2}{(\alpha^2 + \lambda^2)} J_0(B\alpha) J_1(t\alpha) d\alpha = -\lambda K_0(B\lambda) I_1(t\lambda) \quad (B \geq t)$$

$$\int_0^{\infty} \frac{\alpha}{(\alpha^2 + \lambda^2)^2} J_0(B\alpha) J_0(t\alpha) d\alpha = \frac{1}{2\lambda} [BK_1(B\lambda)I_0(t\lambda) - tK_0(B\lambda)I_1(t\lambda)] \quad (B \geq t)$$

$$\int_0^{\infty} \frac{\alpha^2}{(\alpha^2 + \lambda^2)^2} J_1(B\alpha) J_0(t\alpha) d\alpha \quad (B \geq t)$$

$$= \frac{1}{2\lambda} [B\lambda K_0(B\lambda)I_0(t\lambda) - t\lambda K_1(B\lambda)I_1(t\lambda)]$$

$$\int_0^{\infty} \frac{\alpha}{(\alpha^2 + \lambda^2)^2} J_1(B\alpha) J_1(t\alpha) d\alpha \quad (B \geq t)$$

$$= \frac{1}{2\lambda} \left[ BK_0(B\lambda)I_1(t\lambda) + \frac{2}{\lambda} K_1(B\lambda)I_1(t\lambda) - \frac{1}{2\lambda} tK_1(B\lambda)I_0(t\lambda) \right]$$

$$\int_0^{\infty} \frac{\alpha^2}{(\alpha^2 + \lambda^2)^2} J_0(B\alpha) J_1(t\alpha) d\alpha \quad (B \geq t)$$

$$= \frac{1}{2\lambda} [-B\lambda K_1(B\lambda)I_1(t\lambda) + t\lambda K_0(B\lambda)I_0(t\lambda)]$$

## APPENDIX B

### INTEGRAL FORMS AND COEFFICIENTS

$E_1, E_2, E_3$  and  $E_4$  integrals are given as

$$E_1 = -\frac{1}{(K+1)} \int_a^b f(t)t [(K+1)I_1(t\lambda)K_1(B\lambda) + 2\lambda BI_1(t\lambda)K_0(B\lambda) - 2\lambda tI_0(t\lambda)K_1(B\lambda)] dt$$

$$E_2 = -\frac{1}{(K+1)} \int_a^b f(t)t [-2t\lambda I_0(t\lambda)K_0(B\lambda) - (K+1)I_1(t\lambda)K_0(B\lambda) + 2B\lambda I_1(t\lambda)K_1(B\lambda)] dt$$

$$E_3 = -\frac{1}{(K+1)} \int_a^b f(t)t \left[ -4(tI_0(A\lambda)K_0(t\lambda) - AI_1(A\lambda)K_1(t\lambda))\lambda^2 + \frac{4(tI_1(A\lambda)K_0(t\lambda) - AI_1(A\lambda)K_0(t\lambda))\lambda}{A} + \frac{2(K+1)I_1(A\lambda)K_1(t\lambda)}{A} \right] dt$$

$$E_4 = -\frac{1}{(K+1)} \int_a^b f(t)t \left[ \frac{1}{2}\lambda^2 (AI_0(A\lambda)K_1(t\lambda) - tI_1(A\lambda)K_0(t\lambda)) \right] dt$$

$l_{11} - l_{44}$  coefficients are given as

$$l_{11} = \left( 2AB(H_{01}K_0(A\lambda) - H_{11}K_1(A\lambda)) - \frac{2AK_0(B\lambda)}{\lambda} \right) \lambda^4 + \left( 2A(K+1)(H_{00}K_0(A\lambda) - H_{10}K_1(A\lambda)) + \frac{B(K+1)K_1(B\lambda)}{A\lambda} \right) \lambda^3 + \left( -\frac{(K+1)(K+3)K_0(B\lambda)}{2A\lambda} - \frac{BH_{11}(K+1)K_1(A\lambda)}{A} \right) \lambda^2 - \frac{H_{10}(K+1)^2K_1(A\lambda)\lambda}{A}$$

$$l_{12} = \left( 2AB(H_{00}K_0(A\lambda) - H_{10}K_1(A\lambda)) + \frac{2AK_1(B\lambda)}{\lambda} \right) \lambda^4 + \left( \frac{(1-K^2)K_1(B\lambda)}{2A\lambda} - \frac{BH_{10}(K+1)K_1(A\lambda)}{A} \right) \lambda^2 - \frac{B(K+1)K_0(B\lambda)\lambda^2}{A}$$

$$\begin{aligned}
l_{13} = & \left( AB(H_{00}K_0(B\lambda) - H_{01}K_1(B\lambda)) - \frac{BK_1(A\lambda)}{\lambda} \right) \lambda^3 \\
& + \left( A(K+1)H_{00}K_1(B\lambda) - \frac{1}{2}B(K+1)(H_{10}K_0(B\lambda) + H_{11}K_1(B\lambda)) \right) \lambda^2 \\
& - \frac{1}{2}(K+1)^2H_{10}\lambda K_1(B\lambda)
\end{aligned}$$

$$\begin{aligned}
l_{14} = & \left( \frac{BK_0(A\lambda)}{\lambda} - AB(H_{10}K_0(B\lambda) + H_{11}K_1(B\lambda)) \right) \lambda^3 \\
& + \left( \frac{BK_1(A\lambda)}{A\lambda} + \frac{1}{2}B(K-1)(H_{10}K_0(B\lambda) + H_{01}K_1(B\lambda)) \right. \\
& \left. - A(K+1)H_{10}K_1(B\lambda) \right) \lambda^2 + \frac{1}{2}(K^2-1)H_{00}K_1(B\lambda)
\end{aligned}$$

$$\begin{aligned}
l_{21} = & \left( -2ABH_{01}I_0(B\lambda) + \frac{2AI_0(B\lambda)}{\lambda} - 2ABH_{11}I_1(A\lambda) \right) \lambda^4 \\
& + \left( -2AH_{00}I_0(A\lambda)(K+1) - 2AH_{10}I_1(A\lambda)(K+1) \right. \\
& \left. + \frac{BI_1(B\lambda)}{A\lambda}(K+1) \right) \lambda^3 + \left( \frac{(K^2+4K+3)I_0(B\lambda)}{2A\lambda} - \frac{BH_{11}I_1(A\lambda)}{A} \right) \lambda^2 \\
& - \frac{H_{10}(K+1)^2I_1(A\lambda)\lambda}{A}
\end{aligned}$$

$$\begin{aligned}
l_{22} = & \left( -2ABH_{00}I_0(A\lambda) - 2AH_{10}I_1(A\lambda) + \frac{2AI_1(B\lambda)}{\lambda} \right) \lambda^4 \\
& + \left( -\frac{BH_{10}I_1(A\lambda)}{A} - \frac{BH_{10}KI_1(A\lambda)}{A} + \frac{(1-K^2)I_1(B\lambda)}{2A\lambda} \right) \lambda^2 \\
& + \frac{B(K+1)I_0(B\lambda)\lambda^2}{A}
\end{aligned}$$

$$\begin{aligned}
l_{23} = & \left( -ABH_{00}I_0(B\lambda) - \frac{BI_1(A\lambda)}{\lambda} + ABH_{01}I_1(B\lambda) \right) \lambda^3 \\
& + \left( \frac{1}{2}BH_{10}(K+1)I_0(B\lambda) + AH_{00}(K+1)I_1(B\lambda) \right. \\
& \left. - \frac{1}{2}BH_{11}(K+1)I_1(B\lambda) \right) \lambda^2 - \frac{1}{2}BH_{10}(K+1)I_1(B\lambda)\lambda
\end{aligned}$$

$$\begin{aligned}
l_{24} &= \left( -ABH_{11}I_1(B\lambda) - \frac{BI_0(A\lambda)}{\lambda} + ABH_{10}I_0(B\lambda) \right) \lambda^3 \\
&\quad + \left( \frac{1}{2}BH_{01}(K-1)I_1(B\lambda) - AH_{10}(K+1)I_1(B\lambda) \right. \\
&\quad \left. - \frac{1}{2}BH_{00}(K-1)I_0(B\lambda) + \frac{BI_0(A\lambda)}{A\lambda} \right) \lambda^2 - \frac{1}{2}H_{00}(K^2-1)I_1(B\lambda)\lambda \\
l_{31} &= \left( AH_{00}K_0(A\lambda) - AH_{10}K_1(A\lambda) + \frac{BK_1(B\lambda)}{A\lambda} \right) \lambda^3 - \frac{(K+1)K_0(B\lambda)\lambda}{2A} \\
&\quad - \frac{H_{10}(K+1)K_1(A\lambda)\lambda}{2A} \\
l_{32} &= \left( AH_{01}K_0(A\lambda) - AH_{11}K_1(A\lambda) - \frac{BK_0(B\lambda)}{A\lambda} \right) \lambda^3 - \frac{(K+1)K_1(B\lambda)\lambda}{2A} \\
&\quad - \frac{H_{11}(K+1)K_1(A\lambda)\lambda}{2A} \\
l_{33} &= \left( \frac{AK_0(A\lambda)}{2B\lambda} - \frac{1}{2}BH_{10}K_0(B\lambda) - \frac{1}{2}BH_{11}K_1(B\lambda) \right) \lambda^2 \\
&\quad + \frac{1}{4}(K+1)(H_{11}K_0(B\lambda) - H_{10}K_1(B\lambda))\lambda \\
l_{34} &= \left( \frac{1}{2}BH_{00}K_0(B\lambda) - \frac{AK_1(A\lambda)}{2B\lambda} + \frac{1}{2}BH_{01}K_1(B\lambda) \right) \lambda^2 \\
&\quad + \left( -\frac{K_0(A\lambda)}{4B\lambda} - \frac{1}{2}H_{01}K_0(B\lambda) + \frac{BH_{10}K_0(B\lambda)}{2A} - \frac{1}{4}H_{01}KK_0(B\lambda) \right. \\
&\quad \left. + \frac{BH_{11}K_1(B\lambda)}{2A} + \frac{1}{4}H_{00}KK_1(B\lambda) \right) \lambda - \frac{H_{11}(K+1)K_0(B\lambda)}{2A} \\
l_{41} &= \left( -AH_{00}I_0(A\lambda) - AH_{10}I_1(A\lambda) + \frac{BI_1(B\lambda)}{A\lambda} \right) \lambda^3 - \frac{(K+1)I_0(B\lambda)\lambda}{2A} \\
&\quad - \frac{H_{10}(K+1)I_1(A\lambda)\lambda}{2A} \\
l_{42} &= \left( -AH_{01}I_0(A\lambda) - AH_{11}I_1(A\lambda) + \frac{BI_0(B\lambda)}{A\lambda} \right) \lambda^3 - \frac{I_1(B\lambda)\lambda}{2A} - \frac{H_{11}(K+1)I_1(A\lambda)\lambda}{2A} \\
l_{43} &= \left( -\frac{AI_0(A\lambda)}{2B\lambda} + \frac{1}{2}BH_{10}I_0(B\lambda) - \frac{1}{2}BH_{11}I_1(B\lambda) \right) \lambda^2 \\
&\quad + \frac{1}{4}(-K-1)(H_{11}I_0(B\lambda) + H_{10}I_1(B\lambda))\lambda
\end{aligned}$$

$$\begin{aligned}
l_{44} = & \left( -\frac{1}{2}BH_{00}I_0(B\lambda) - \frac{AI_1(A\lambda)}{2B\lambda} + \frac{1}{2}BH_{01}I_1(B\lambda) \right) \lambda^2 \\
& + \left( \frac{I_0(A\lambda)}{4B\lambda} + \frac{1}{2}H_{01}I_0(B\lambda) - \frac{BH_{10}I_0(B\lambda)}{2A} + \frac{1}{4}H_{01}KI_0(B\lambda) \right. \\
& \left. + \frac{BH_{11}I_1(B\lambda)}{2A} + \frac{1}{4}H_{00}KI_1(B\lambda) \right) \lambda + \frac{H_{11}(K+1)I_0(B\lambda)}{2A}
\end{aligned}$$

$D$  is given as

$$\begin{aligned}
D = & ABK_1(A\lambda)^2I_0(B\lambda)^2\lambda^4 - ABI_1(B\lambda)^2K_0(A\lambda)^2\lambda^4 + ABI_0(A\lambda)^2K_0(B\lambda)^2\lambda^4 \\
& - ABI_1(A\lambda)^2K_0(B\lambda)^2\lambda^4 - ABI_0(B\lambda)^2K_1(A\lambda)^2\lambda^4 \\
& + ABI_1(B\lambda)^2K_1(A\lambda)^2\lambda^4 - ABI_0(A\lambda)^2K_1(B\lambda)^2\lambda^4 \\
& + ABI_1(A\lambda)^2K_1(B\lambda)^2\lambda^4 - 2ABI_0(A\lambda)I_0(B\lambda)K_0(A\lambda)K_0(B\lambda)\lambda^4 \\
& - 2ABI_0(B\lambda)I_1(A\lambda)K_0(B\lambda)K_1(A\lambda)\lambda^4 \\
& - 2ABI_0(A\lambda)I_1(B\lambda)K_0(A\lambda)K_1(B\lambda)\lambda^4 \\
& - 2ABI_1(A\lambda)I_1(B\lambda)K_1(A\lambda)K_1(B\lambda)\lambda^4 - AI_0(B\lambda)I_1(B\lambda)K_0(A\lambda)^2\lambda^3 \\
& - AKI_0(B\lambda)I_1(B\lambda)K_0(A\lambda)^2\lambda^3 + AKI_0(B\lambda)I_1(B\lambda)K_1(A\lambda)^2\lambda^3 \\
& + AI_0(A\lambda)I_1(B\lambda)K_0(A\lambda)K_0(B\lambda)\lambda^3 \\
& + AKI_0(A\lambda)I_1(B\lambda)K_0(A\lambda)K_0(B\lambda)\lambda^3 \\
& - AI_1(A\lambda)I_1(B\lambda)K_0(A\lambda)K_0(B\lambda)\lambda^3 + AKI_1(A\lambda)I_1(B\lambda)K_0(B\lambda)K_1(A\lambda)\lambda^3 \\
& + AI_0(A\lambda)I_0(B\lambda)K_0(A\lambda)K_1(B\lambda)\lambda^3 \\
& - AKI_0(A\lambda)I_0(B\lambda)K_0(A\lambda)K_1(B\lambda)\lambda^3 - AI_0(A\lambda)^2K_0(B\lambda)K_1(B\lambda)\lambda^3 \\
& + AKI_0(A\lambda)^2K_0(B\lambda)K_1(B\lambda)\lambda^3 - AI_0(A\lambda)I_0(B\lambda)K_0(A\lambda)K_1(B\lambda)\lambda^3 \\
& + AKI_1(A\lambda)^2K_0(B\lambda)K_1(B\lambda)\lambda^3 + AI_0(A\lambda)I_1(A\lambda)K_0(B\lambda)K_1(B\lambda)\lambda^3 \\
& + AI_0(A\lambda)I_0(B\lambda)K_1(A\lambda)K_1(B\lambda)\lambda^3 - AKI_0(B\lambda)I_1(A\lambda)K_1(A\lambda)K_1(B\lambda)\lambda^3 \\
& - \frac{BI_1(A\lambda)^2K_0(B\lambda)^2\lambda^2}{2A} - \frac{BK I_1(A\lambda)^2K_0(B\lambda)^2\lambda^2}{2A} - \frac{BI_0(B\lambda)^2K_1(A\lambda)^2\lambda^2}{2A} \\
& - \frac{BK I_0(B\lambda)^2K_1(A\lambda)^2\lambda^2}{2A} + \frac{BI_1(B\lambda)^2K_1(A\lambda)^2\lambda^2}{2A} \\
& + \frac{BK I_1(B\lambda)^2K_1(A\lambda)^2\lambda^2}{2A} + \frac{BI_1(A\lambda)^2K_1(B\lambda)^2\lambda^2}{2A} \\
& + \frac{BK I_1(A\lambda)^2K_1(B\lambda)^2\lambda^2}{2A} + \frac{B\lambda^2}{A} - \frac{BI_0(B\lambda)I_1(A\lambda)K_0(B\lambda)K_1(A\lambda)\lambda^2}{A}
\end{aligned}$$

$$\begin{aligned}
& - \frac{BI_0(B\lambda)I_1(A\lambda)K_0(B\lambda)K_1(A\lambda)\lambda^2}{A} - \frac{BI_1(A\lambda)I_1(B\lambda)K_1(A\lambda)K_1(B\lambda)\lambda^2}{A} \\
& - \frac{BK I_1(A\lambda)I_1(B\lambda)K_1(A\lambda)K_1(B\lambda)\lambda^2}{A} + \frac{A\lambda^2}{B} \\
& + \frac{K^2 I_0(B\lambda)I_1(B\lambda)K_1(A\lambda)^2\lambda}{2A} + \frac{K I_0(B\lambda)I_1(B\lambda)K_1(A\lambda)^2\lambda}{A} \\
& + \frac{I_0(B\lambda)I_1(B\lambda)K_1(A\lambda)^2\lambda}{2A} + \frac{K^2 I_1(A\lambda)I_1(B\lambda)K_0(B\lambda)K_1(A\lambda)\lambda}{2A} \\
& + \frac{K I_1(A\lambda)I_1(B\lambda)K_0(B\lambda)K_1(A\lambda)\lambda}{A} + \frac{I_1(A\lambda)I_1(B\lambda)K_0(B\lambda)K_1(A\lambda)\lambda}{2A} \\
& - \frac{K^2 I_1(A\lambda)^2 K_0(B\lambda)K_1(B\lambda)\lambda}{2A} - \frac{K I_1(A\lambda)^2 K_0(B\lambda)K_1(B\lambda)\lambda}{A} \\
& - \frac{I_1(A\lambda)^2 K_0(B\lambda)K_1(B\lambda)\lambda}{2A} - \frac{K^2 I_0(B\lambda)I_1(A\lambda)K_1(A\lambda)K_1(B\lambda)\lambda}{2A} \\
& - \frac{K I_0(B\lambda)I_1(A\lambda)K_1(A\lambda)K_1(B\lambda)\lambda}{A} - \frac{I_0(B\lambda)I_1(A\lambda)K_1(A\lambda)K_1(B\lambda)\lambda}{2A} \\
& + \frac{K^2}{4AB} + \frac{K}{AB} + \frac{3}{4AB}
\end{aligned}$$

where

$$H_{ij}(\lambda A, \lambda B) = K_i(\lambda A)I_j(\lambda B) + (-1)^{i+j+1}I_i(\lambda A)K_j(\lambda B) \quad (i, j = 0, 1)$$



## APPENDIX C

### ASYMPTOTIC EXPANSIONS

Asymptotic expansions for modified Bessel functions for  $\lambda \rightarrow \infty$  (Abramowitz and Stegun 1965)

$$K_1(B\lambda) \sim \frac{e^{-\lambda B} \sqrt{\pi}}{\sqrt{2\lambda B}} \left( 1 + \frac{3}{8\lambda B} - \frac{15}{128\lambda^2 B^2} \right)$$

$$K_1(t\lambda) \sim \frac{e^{-\lambda t} \sqrt{\pi}}{\sqrt{2\lambda t}} \left( 1 + \frac{3}{8\lambda t} - \frac{15}{128\lambda^2 t^2} \right)$$

$$K_1(A\lambda) \sim \frac{e^{-\lambda A} \sqrt{\pi}}{\sqrt{2\lambda A}} \left( 1 + \frac{3}{8\lambda A} - \frac{15}{128\lambda^2 A^2} \right)$$

$$K_1(r\lambda) \sim \frac{e^{-\lambda r} \sqrt{\pi}}{\sqrt{2\lambda r}} \left( 1 + \frac{3}{8\lambda r} - \frac{15}{128\lambda^2 r^2} \right)$$

$$K_0(B\lambda) \sim \frac{e^{-\lambda B} \sqrt{\pi}}{\sqrt{2\lambda B}} \left( 1 - \frac{1}{8\lambda B} + \frac{9}{128\lambda^2 B^2} \right)$$

$$K_0(t\lambda) \sim \frac{e^{-\lambda t} \sqrt{\pi}}{\sqrt{2\lambda t}} \left( 1 - \frac{1}{8\lambda t} + \frac{9}{128\lambda^2 t^2} \right)$$

$$K_0(A\lambda) \sim \frac{e^{-\lambda A} \sqrt{\pi}}{\sqrt{2\lambda A}} \left( 1 - \frac{1}{8\lambda A} + \frac{9}{128\lambda^2 A^2} \right)$$

$$K_0(r\lambda) \sim \frac{e^{-\lambda r} \sqrt{\pi}}{\sqrt{2\lambda r}} \left( 1 - \frac{1}{8\lambda r} + \frac{9}{128\lambda^2 r^2} \right)$$

$$I_1(B\lambda) \sim \frac{e^{\lambda B}}{\sqrt{2\pi\lambda B}} \left( 1 - \frac{3}{8\lambda B} - \frac{15}{128\lambda^2 B^2} \right)$$

$$I_1(t\lambda) \sim \frac{e^{\lambda t}}{\sqrt{2\pi\lambda t}} \left( 1 - \frac{3}{8\lambda t} - \frac{15}{128\lambda^2 t^2} \right)$$

$$I_1(A\lambda) \sim \frac{e^{\lambda A}}{\sqrt{2\pi\lambda A}} \left( 1 - \frac{3}{8\lambda A} - \frac{15}{128\lambda^2 A^2} \right)$$

$$I_1(r\lambda) \sim \frac{e^{\lambda r}}{\sqrt{2\pi\lambda r}} \left( 1 - \frac{3}{8\lambda r} - \frac{15}{128\lambda^2 r^2} \right)$$

$$I_0(B\lambda) \sim \frac{e^{\lambda B}}{\sqrt{2\pi\lambda B}} \left( 1 + \frac{1}{8\lambda B} + \frac{9}{128\lambda^2 B^2} \right)$$

$$I_0(t\lambda) \sim \frac{e^{\lambda t}}{\sqrt{2\pi\lambda t}} \left( 1 + \frac{1}{8\lambda t} + \frac{9}{128\lambda^2 t^2} \right)$$

$$I_0(A\lambda) \sim \frac{e^{\lambda A}}{\sqrt{2\pi\lambda A}} \left( 1 + \frac{1}{8\lambda A} + \frac{9}{128\lambda^2 A^2} \right)$$

$$I_0(r\lambda) \sim \frac{e^{\lambda r}}{\sqrt{2\pi\lambda r}} \left( 1 + \frac{1}{8\lambda r} + \frac{9}{128\lambda^2 r^2} \right)$$

## APPENDIX D

### ALGEBRAIC EQUALITIES

$$\begin{aligned}\frac{(B-r)(B-t)}{(2B-r-t)^3} &= \frac{(B-r)}{(2B-r-t)^2} - \frac{(B-r)^2}{(2B-r-t)^3} \\ \frac{(B-t)}{(2B-r-t)^2} &= \frac{1}{(2B-r-t)} - \frac{(B-r)}{(2B-r-t)^2} \\ \frac{(A-r)(A-t)}{(-2A+r+t)^3} &= -\frac{(A-r)}{(2A-r-t)^2} + \frac{(A-r)^2}{(2A-r-t)^3} \\ \frac{(A-t)}{(-2A+r+t)^2} &= \frac{1}{(2A-r-t)} - \frac{(A-r)}{(2A-r-t)^2} \\ \frac{1}{(2B-r-t)^3} &= -\frac{1}{2} \frac{d^2}{dr^2} \left[ \frac{1}{(t+r-2B)} \right] \\ \frac{1}{(2B-r-t)^3} &= -\frac{1}{2} \frac{d}{dr} \frac{1}{(t+r-2B)}\end{aligned}$$

## APPENDIX E

### GAUSS-LOBATTO AND GAUSS-LAGUERRE INTEGRATION

Gauss-Lobatto integration formula

$$\frac{1}{\pi} \int_{-1}^1 \frac{f(t)}{\sqrt{1-t^2}} w(t) dt = \sum_{i=1}^n C_i f(t_i) w(t_i)$$

where

$$t_i = \cos \left[ \frac{(i-1)\pi}{(n-1)} \right] \quad (i = 1, 2, 3, \dots, n)$$

$$C_i = \frac{1}{n-1} \quad (i = 2, 3, 4, \dots, n-1)$$

$$C_1 = C_n = \frac{1}{2(n-1)}$$

Gauss-Laguerre integration formula

$$\int_0^{\infty} f(t) dt = \int_0^{\infty} e^{-t} [e^t f(t)] dt \approx \sum_{i=1}^n w(t_i) e^t f(t_i)$$

where  $t_i$  are abscissas and  $w(t_i)$  are weights of the Laguerre integration.